The δ^{53}Cr isotope composition of komatiite flows and implications for the composition of the bulk silicate Earth

Matthew Jerram[a,b*], Pierre Bonnand[c], Andrew C. Kerr[d], Euan G. Nisbet[e], Igor S. Puchtel[f] and Alex N. Halliday[b]

[a]Department of Earth Sciences, University of Oxford, Oxford OX1 3AN, UK
[b]The Earth Institute, Columbia University, New York, NY, 10025 USA
[c]Laboratoire Magmas et Volcans, Université Clermont Auvergne, CNRS, Clermont-Ferrand, France.
[d]School of Earth and Ocean Sciences, Cardiff University, Cardiff CF10 3AT, Wales, UK
[e]Department of Earth Sciences, Royal Holloway, University of London, Egham TW20 0EX, UK
[f]Department of Geology, University of Maryland, 8000 Regents Drive, College Park, MD 20742, USA

Revised for: *Chemical Geology*

Version: April 07, 2020

*Corresponding author: matthew.jerram@columbia.edu

Abstract

Data on the chromium stable isotope composition of planetary reservoirs have the potential to provide information about core formation, partial melting and conditions of the Moon formation. In order to detect the small Cr isotopic differences between various reservoirs in the solar system, their compositions need to be precisely constrained. The current BSE value of $\delta^{53}Cr$= -0.11 ± 0.06‰ (Sossi et al., 2018) cannot resolve differences between achondrites, (Vesta $\delta^{53}Cr$= -0.17 ± 0.05‰) and chondrites (carbonaceous $\delta^{53}Cr$= -0.12 ± 0.05 ‰; ordinary $\delta^{53}Cr$= -0.11 ± 0.04 ‰). The composition of the bulk silicate Earth (BSE) is often used as a reference point for comparisons to other planetary reservoirs. However, past attempts to estimate the Cr isotopic composition of the BSE have been unable to provide a well-constrained BSE value. Traditional methods, using mantle peridotites, are affected by the susceptibility of Cr isotopes to fractionation during metasomatism. More recently, the Cr isotope composition of the BSE has been calculated using komatiites, in addition to mantle peridotites, to produce a more precise value (Sossi et al., 2018). In order to constrain the BSE composition to a higher precision, the $\delta^{53}Cr$ of remarkably fresh komatiite lava flows from three localities, ranging in age from 2.7 Ga to 89 Ma, have been investigated in detail. These included the Tony's Flow in the Belingwe Greenstone Belt, Zimbabwe, the Victoria's Lava Lake in Fennoscandia, and komatiites from Gorgona Island in Colombia.

In the komatiites studied, a range in Cr isotopic compositions was found, from $\delta^{53}Cr$ = -0.16 ± 0.02 to -0.01 ± 0.02 ‰. We show that the high degrees of partial melting that produced the komatiites, did not result in Cr isotopic fractionation between the komatiitic melt and mantle residue. However, limited Cr isotopic fractionation is found to be a consequence of komatiite lava differentiation. For the lava flows with high Mg content and high $Cr^{2+}/\Sigma Cr_{TOT}$ (the molar ratio of $Cr^{2+}/(Cr^{2+} + Cr^{3+})$, such as Tony's Flow and Gorgona, $\delta^{53}Cr$ increases in the evolved portion of the magma during olivine fractionation due

to the preferential inclusion of light Cr into olivine. Other flows with lower MgO content do not show this behaviour because a smaller fraction of the Cr is contained in olivine. The effects of fractional crystallisation must, therefore, be taken into account when calculating the Cr isotopic composition of the source of komatiite lavas.

The weighted average of $\delta^{53}Cr$ for the komatiite lavas analysed is -0.12 ± 0.04 ‰ (n=5) and represents our best estimate for the Cr isotopic composition of the BSE. It agrees with the previous estimates, while providing an improvement to the uncertainty. There is no resolvable difference between this value and that of chondritic meteorites. Our data also indicate that the $\delta^{53}Cr$ of the mantle has been constant since at least the Archean.

Keywords:
Cr stable isotopes; komatiites; mantle melting; fractional crystallisation; Bulk Silicate Earth.

1. Introduction

Variations in stable isotope ratios provide a powerful tool for exploring planetary interiors. The composition of the bulk silicate Earth (BSE) is often used as a reference relative to which differences between reservoirs can be identified. For example, comparison of the Si isotope compositions of chondrites and the BSE showed that Si isotopes fractionated during core formation (Armytage et al., 2011; Shahar et al., 2009), whereas the different K isotope compositions of the BSE and the lunar mantle likely indicate that K was lost during the Moon-forming impact (Wang and Jacobsen, 2016).

Several recent studies have explored the Cr isotope composition of reservoirs in the Solar System and on Earth. The stable chromium isotope composition of planetary reservoirs has received attention due to the variable geochemical nature of Cr, which means that its isotopic composition may record information about a range of processes. For instance, Cr can be lithophile or siderophile, depending upon the oxygen fugacity and temperature (Fischer et al., 2015; Siebert et al., 2011; Wood et al., 2008); it can also be compatible or incompatible during mantle melting depending on its oxidation state (Li et al., 1995; Roeder and Reynolds, 1991; Schreiber and Haskin, 1976). The geochemical behaviour of Cr is expected to be recorded in the stable Cr isotope composition.

Chromium stable isotope variations are presented using the delta notation, defined as per mil deviations from the NIST 979 standard (Ellis et al., 2002). Previous studies have investigated the behaviour of Cr stable isotopes in a range of settings. Terrestrial core formation did not fractionate the stable Cr isotope composition, as there is no resolvable difference between the δ^{53}Cr composition of the mantle and chondrites (Bonnand et al., 2016b; Schoenberg et al., 2016). However, crystallisation within planetesimal cores (iron meteorites) can lead to variations in δ^{53}Cr, which can be used to identify the oxygen fugacity during metal-silicate partitioning of the bodies they formed in (Bonnand and Halliday, 2018). Lunar basalts show a small difference compared to the composition of the BSE (Bonnand et al.,

2016a; Sossi et al., 2018), which has been linked to the loss of heavy Cr isotopes to an oxidised gas in the lunar magma ocean. Other planetary bodies, such as Vesta, are also isotopically light compared to Earth, which is explained by volatile loss of Cr (Zhu et al., 2019). In order to accurately identify and interpret variations in Cr isotope data from other reservoirs, a well constrained value for the BSE is required.

Different methods are available for estimating the stable element isotopic composition of the BSE, with the best method dependent upon the behaviour of a particular element. The highly incompatible element isotope compositions can be estimated using crustal samples, as the crust is where the majority of these elements reside in the BSE, (e.g., the BSE composition of $\delta^{41}K$ can be estimated by analysing basalts from different tectonic settings; (Tuller-Ross et al., 2019). In contrast, Cr is a compatible element during mantle melting, with > 99 % of the BSE reservoir contained in the mantle (e.g., Xia et al., 2017). As such, samples representative of the mantle must be used.

Peridotites are often used to study the composition of the BSE, as they provide direct samples of the mantle. The first BSE $\delta^{53}Cr$ value was obtained from the average Cr isotopic composition of mantle peridotites ($\delta^{53}Cr$ = -0.12 ± 0.10 ‰, n = 24; Schoenberg et al. 2008). Xia et al. (2017) subsequently used a filtered set of mantle peridotites, to avoid the effects of partial melting, and these yielded a similar value of -0.14 ± 0.12 ‰, (n = 12). However, $\delta^{53}Cr$ values of mantle peridotites are often affected by cryptic metasomatism (Xia et al., 2017, Shen et al., 2018), the effects of which can be difficult to identify and correct for.

Another method used to estimate the stable isotope composition of the BSE is to use the primary composition of komatiite lavas (e.g., Badullovich et al., 2017; Dauphas et al., 2010; Gall et al., 2017; Greber et al., 2015). Komatiites are high degree partial melts that were derived from melting at temperatures significantly higher than those of the ambient mantle (Arndt et al., 1997, 1998; Arndt and Nisbet, 1982; Green, 1975; Kushiro and Yoder, 1969). The high degrees of melting mean that the

komatiite melt composition approaches that of the mantle peridotite. Furthermore, komatiite melts sample a large volume of the mantle, therefore, small-scale metasomatic variations within the mantle sources of komatiites were likely to be averaged out. Sossi et al. (2018) used a filtered mantle peridotite and komatiite set of samples to produce a more tightly constrained $\delta^{53}Cr$ value for the BSE of -0.11 ± 0.06 (n = 36). Komatiites with A_1 or A_2 spinifex zone textures were chosen, as these parts of lava flows were considered to have compositions closest to those of their primary magmas (Faure et al., 2006; Sossi et al., 2016). It is important that the Cr isotopic composition of komatiite samples used in these studies are representative of the primary komatiite melt; this, in turn, requires understanding of the behaviour of Cr during differentiation of komatiite lava flows. Further complications may arise from post-magmatic modifications, such as seafloor alteration and metamorphism, and the effects these processes may have had on the $\delta^{53}Cr$ of komatiites.

Chromium behaviour in komatiites diverges from other silicate melts. Komatiites contain higher Cr abundances (1000 – 3000 μg g^{-1}) than other melts; e.g., basalts typically contain < 500 μg g^{-1} Cr (Basaltic Volcanism Study Project, 1981). The amount of Cr in silicate melts is limited by the low solubility of Cr^{3+} (Hanson and Jones, 1998). Higher formation temperatures of komatiites create higher $Cr^{2+}/\Sigma Cr_{TOT}$ and melts of different compositions, which increases the amount of total Cr that can be dissolved in the melt (Berry et al., 2006; Li et al., 1995; Schreiber and Haskin, 1976; Sossi and O'Neill, 2016). In komatiites, this occurs concurrently with high degree partial melting, which exhausts the major Cr bearing phases, releasing more Cr into the melt (e.g., Walter, 1998). In komatiite flows, Cr is contained within two minerals, chromite (Barnes, 1998) and chromium rich olivine (500-2000 μg g^{-1}, Arndt, 2008). The high Cr contents of olivine can be the result of high Cr concentrations in the melt, elevated $Cr^{2+}/\Sigma Cr_{TOT}$ of the melt, and delayed crystallisation of chromite (Donaldson, 1982; Shore, 1996). Delayed chromite crystallisation will occur if melt is undersaturated in Cr. Chromium saturation is controlled by the Mg content and the oxidation state of a komatiite melt (Barnes, 1998; Murck and

Campbell, 1986). Fractional crystallisation of olivine and chromite leads to a distinct evolution of the Cr contents in komatiite flows, as described in Arndt (2008) and shown in Figure 1. Initial olivine crystallisation and accumulation leads to an increase in Cr of the residual melt, followed by a decrease once chromite crystallisation begins. Variations in Cr isotope composition may be affected by crystallisation of these phases.

Variations in δ^{53}Cr during fractional crystallisation of silicate melts have previously been identified (Bonnand et al., 2020, 2016a). In lunar basalts, crystallisation of isotopically heavy oxides leads to decreasing δ^{53}Cr in the melt (Bonnand et al., 2016a). A similar trend is seen in ocean island basalts, where crystallisation of pyroxene and spinel leads to decreasing δ^{53}Cr variations in the melt (Bonnand et al., 2020). The magmatic evolution of δ^{53}Cr in komatiites may also differ due to the higher Cr concentration in these melts, the higher liquidus temperatures, and the minerals that host Cr.

It is important that the emplaced komatiite lava composition is representative of that of the mantle. The effect of partial melting on δ^{53}Cr has been debated in previous studies, with only small fractionations expected in basalts (< 0.1 ‰, Shen et al. 2018, 2019; Bonnand et al., 2020). The higher liquidus temperatures and greater degrees of partial melting at which komatiites form may be expected to lead to even smaller fractionations. Indeed, Sossi et al. (2018) found no difference in δ^{53}Cr between the compositions of komatiites and mantle peridotites. Therefore, komatiites can be regarded as valuable probes of the Cr isotope composition of the mantle. Komatiites in this study have also been affected by non-magmatic processes that might be able to alter the δ^{53}Cr of silicate rocks (e.g. Farkaš et al., 2013; Frei et al., 2014). The effect that processes, such as weathering, serpentinisation, and crustal contamination, could have had on the δ^{53}Cr of komatiites, must be considered.

In order to further improve the estimates of the δ^{53}Cr of the BSE using komatiites, it is necessary to fully understand the behaviour of Cr in these lavas. Fractionations that occur in komatiites will

depend upon the minerals present, and whether Cr behaved compatibility or incompatibility in these minerals will affect the choice of samples when calculating the emplaced komatiite lava composition. Previously, A_1 and A_2 spinifex-textured komatiite samples have been used to represent the composition of the emplaced lava. Typically, A_1 and A_2 spinifex-textured komatiites show a range in MgO content within lava flows, and, therefore, they may represent various stages in the evolution of the melt. Whether these komatiite samples are representative of the emplaced komatiite lava will depend on how Cr behaved during crystallisation. In this contribution, the effects of crystallisation on Cr isotopic composition is considered for the first time through a detailed examination of three exceptionally well preserved komatiite systems, i.e., Gorgona Island, Tony's Flow, and Victoria's Lava Lake. This information is used to provide a new estimate for the Cr isotopic composition of the BSE.

2. Samples

2.1. Tony's Flow, Belingwe

Tony's Flow is part of the 0.5 to 1 km thick Reliance Formation, from the Belingwe Greenstone Belt (Nisbet et al., 1977), which was emplaced on continental crust in an extensional environment (Bickle et al., 1975; Hunter et al., 1998). The flow has been dated at 2.69 ± 0.01 Ga using the Pb-Pb isotope system on the whole-rock samples (Chauvel et al., 1993). Some parts of the Reliance Group are remarkably well preserved, and a few locations contain mainly primary olivine, and even pristine glass preserved in olivines (Nisbet et al., 1987; Renner et al., 1994). Other minerals within the flow include augite, minor pigeonite, and chromite (Nisbet et al., 1987; Renner et al., 1994).

A total of eight samples from the Tony's Flow were analysed in this study, including five spinifex-textured and three cumulate komatiites from Puchtel et al. (2009). The location of the samples within the flow is illustrated in Puchtel et al. (2009). The komatiites have a range in their chemical composition; MgO varies from 16.5 to 31 wt. % and [Cr] from 2023 to 2455 μg g^{-1}. The MgO concentration of the

parental liquid has been estimated at 24 wt. %, calculated using the composition of melt in equilibrium with the most MgO-rich olivines (Nisbet et al., 1993; Puchtel et al., 2009). The oxygen fugacity of Tony's Flow is estimated at ΔFMQ= +0.48 ± 0.27 (Nicklas et al., 2018). The komatiites from Tony's Flow have been chemically and isotopically well characterised in previous studies (Nisbet et al., 1987; Puchtel et al., 2009; Renner et al., 1994).

2.2. Victoria's Lava Lake, Vetreny Belt

The Victoria's Lava Lake is located in the Vetreny Belt in the Fennoscandian Shield. The komatiites formed as a lava lake (Puchtel et al., 1996), which has been dated at 2407 ± 6 Ma, (Puchtel et al., 1996, 1997, 2016) using the Re-Os internal isochron method. The vetreny belt was formed as part of a large igneous province created by impingement of a mantle plume upon continental crust of the Fennoscandian Shield (Puchtel et al., 1997).

In this study, we used samples from Puchtel et al. (2016). Seven samples were analysed, including four spinifex-textured komatiitic basalts and three olivine cumulates. Pure chromite separates from two of the cumulate samples were also analysed. The only minerals present in the samples as phenocrysts are olivine and chromite. Primary mineralogy is commonly well preserved (Puchtel et al., 1996). Most elements were shown to be immobile within Victoria's Lava Lake during seafloor alteration and metamorphism; the metamorphic grade in the area does not exceed prehnite–pumpellyite facies (Puchtel et al., 1996).

The samples analysed show a range in chemical compositions, with MgO contents varying from 7.4 to 26.6 wt. % and Cr contents from 372 to 3146 μg g^{-1}. While the average composition of the Victoria's Lava Lake is 15 % MgO, the parental magma was estimated to contain ~27 % MgO; it underwent assimilation-fractional crystallisation processes *en route* to the surface (Puchtel et al., 2016). Contamination by tonalites is recognized based on the trace element data, and modelling suggests that

this was on the order of 4 % (Puchtel et al., 2016). The oxidation state of the Victoria's Lava Lake has been estimated at ΔFMQ= +0.43 ± 0.26 (Nicklas et al., 2016, 2018).

2.3. Gorgona Island

Gorgona Island (25 km^2) comprises late Cretaceous basalts, picrites, komatiites, and plutonic rocks located off the west coast of Colombia (Gansser et al., 1979). The suite is related to the Caribbean-Columbian Oceanic Plateau. It is thought to have been generated in an ultra-hot mantle plume (Arndt et al., 1997; Kerr, 2005; Révillon et al., 2000), and was subsequently accreted to the South American continental margin (Arndt et al., 1997). The komatiite samples from Gorgona are of particular interest as they were the first identified komatiite samples from the Phanerozoic (Gansser et al., 1979). The komatiite flows on Gorgona are dated at 89.2 ± 5.2 Ma by the Re-Os method (Walker et al., 1999). The young age of the Gorgona komatiites makes them some of the best preserved globally. Komatiites from Gorgona Island have been well characterised in previous studies (e.g., Arndt et al., 1997; Kerr, 2005; Kerr et al., 1996; Révillon et al., 2000). In this study, we analysed two spinifex-textured and three olivine cumulate samples. The only phenocryst mineral is olivine, which is contained in a groundmass of plagioclase, pyroxene, and chromite (Echeverria, 1980; Kerr et al., 1996). Gorgona Island has poor exposure and is faulted, which obscures the geological relationships of these samples. It is therefore unclear how many lava flows these samples represent. The komatiites analysed in this study have a range of 20.8 to 28.6 wt.% MgO and 514 to 2745 μg g^{-1} Cr and formed from a melt with 22 wt.% MgO. (Arndt et al., 1997).

3. Sample preparation and analytic methods

3.1. Sample Dissolution

Aliquots of sample powders were initially digested in HF and HNO_3 before being slowly dried down to prevent fluoride formation. Residues were then re-dissolved in 6M HCl. If undissolved material remained, high-pressure dissolutions, using a high pressure asher, were carried out. Samples were taken up in 6M HCl and then pressurised within the asher to 100-130 bar and heated to 250°C for 10 hours. The blanks from the high-pressure dissolution were <0.5 ng. The total procedural blank was <1 ng, which was negligible compared to the amount of Cr processed (2 μg).

3.2. Sample Preparation

Aliquots containing two micrograms of Cr were equilibrated with a $^{50\text{-}54}$Cr double spike prior to chemical purification. A two-stage cation exchange column chemistry was used to produce purified Cr. The first column removes matrix elements, while the second column was designed to further remove elements that create isobaric interferences (Ti, V and Fe). An in-depth description of the column procedures is given in Bonnand et al. (2016a). After Cr separation, the samples were treated with H_2O_2 to remove any organic material.

3.3. Thermal Ionisation Mass Spectrometry

A Thermo Scientific Triton thermal ionisation mass spectrometer (TIMS) was used to measure Cr isotopic composition. Chromium was loaded on Re filaments in 6M HCl along with a silicon boride activator. Filaments were flashed to a dull red to ensure that a homogeneous glass was formed. Measurements were made with an ion current of 3-7x10^{-11} A for the largest isotope (^{52}Cr). The cup configuration used allowed all isotopes of Cr (^{50}Cr, ^{52}Cr, ^{53}Cr and ^{54}Cr) and elements with isobaric interferences (^{49}Ti, ^{51}V and ^{56}Fe) to be measured simultaneously in static mode. A single run consisted of

540 ratio acquisitions, with an 8.4 s integration time per ratio. The run was split into 54 blocks, with a 50 s baseline taken after each block. Amplifier gains were measured before each session.

The reproducibility of measurements was calculated by repeat measurements of geological standard JP-1 over a period of one year. This gave a value of $\delta^{53}Cr$= -0.107 ± 0.019‰ (n = 11, 2 s.d.), which agrees well with the results from the previous studies (−0.128 ± 0.022, Bonnand et al., 2016a). The external reproducibility of 19 ppm achieved in this study is comparable or better than those obtained in previous studies (22 ppm (Bonnand et al., 2016a) and 35ppm (Schoenberg et al., 2016)). The internal precision of the individual runs was calculated as 2-times the standard error of the 540 blocks, with a 6 s.e. filter to remove outliers. The external reproducibility of 19 ppm was used to report the uncertainties on the measurements, as it was greater than the internal precision for all measurements.

4. Results

The $\delta^{53}Cr$ compositions of komatiites and chromite separates are reported in Table 1, respectively. Stable Cr isotope compositions of komatiites measured in this study range from $\delta^{53}Cr$ = -0.16 to -0.01 ‰ (Figure 2). There is an overlap between locations and the range in values is similar to that reported in Sossi et al., 2018 ($\delta^{53}Cr$= -0.17 to -0.07 ‰).

Victoria's Lava Lake komatiitic basalts have no resolvable difference between the samples, with a limited $\delta^{53}Cr$ range from -0.16 to -0.14 ‰, despite having a wide range in chemical compositions due to extensive differentiation experienced by the lava lake. No correlation between the Cr isotopic and the chemical composition of the flows implies that the stable Cr isotope composition of this komatiite system was not affected by fractional crystallisation. Chromite separates from two Victoria's Lava Lake komatiite samples were also analysed (12001 and 12105, Table 1 and Figure 3). The Cr isotopic compositions of the chromite separates are identical to those of the bulk rock samples.

The Gorgona Island komatiites have $\delta^{53}Cr$ compositions ranging from -0.15 to -0.06 ‰. These samples do not show as clear a trend between MgO and either [Cr] or $\delta^{53}Cr$ (Figure 2) compared to the other flows in this study. This is explained by the komatiites from Gorgona Island coming from several different lava flows. Two komatiite samples from this locality with the lowest MgO wt. % content have higher $\delta^{53}Cr$ values than the two samples with highest MgO wt. %, which could be explained by fractional crystallisation increasing the $\delta^{53}Cr$ of the residual melt. Komatiite GOR 94-19 has the heaviest Cr isotope composition, which may also be caused due to fractional crystallisation in a separate flow.

Tony's Flow has the largest range in $\delta^{53}Cr$ from -0.14 to -0.01 ‰. There is an increase in $\delta^{53}Cr$ at lower MgO contents, showing that the Cr isotope composition of these komatiites may have been affected by fractional crystallisation. The high MgO komatiite samples, which experienced only olivine fractionation, do not show a clear trend (Figure 2).

5. Discussion

In order to obtain a precise and accurate $\delta^{53}Cr$ value for the BSE using komatiites, within-flow variations in $\delta^{53}Cr$ must be considered. It is important to ensure that the Cr isotopic compositions of the komatiites were not affected by partial melting/fractional crystallization or post-magmatic alteration.

The observed trends between Cr isotope composition and MgO (%) provide evidence that fractional crystallisation indeed effected some of the komatiites studied. This is assessed in detail in the following section.

5.1. Differentiation of komatiite lava flows

Chromium in komatiites is hosted mainly by olivine and chromite, with the distribution between these phases determined by the order and conditions under which these minerals crystallise. Olivine usually contains low concentrations of Cr; in mantle peridotites and mafic lavas the concentration in this phase can be less than 100 μg g^{-1}. However, in komatiites, the Cr concentration in olivine is usually higher (500-2000 μg g^{-1} Arndt, 2008). This is due to a combination of greater compatibility of Cr at high Mg contents, delayed crystallisation of chromite, and higher $Cr^{2+}/\Sigma Cr_{TOT}$ (Donaldson, 1982; Shore, 1996). The higher concentrations in komatiite olivines together with its modal abundance make it a major host of Cr. Chromite is only present in accessory amounts in komatiites, but is also a major host (as shown in Fig. A.1,) as it can contain up to 50 wt. % Cr (the chromites in this study contain less Cr, between 20 to 25 wt. %)

Other mineral phases in komatiites, such as clinopyroxene and sulphide, can contain up to 1000 μg g^{-1} Cr and are predicted to have different $\delta^{53}Cr$ compositions. Sulphides have been calculated to contain isotopically light Cr relative to olivine and chromite (Moynier et al., 2011). In principle, these phases could affect the $\delta^{53}Cr$ evolution of komatiite lavas. However, they are not liquidus phases in komatiites and do not fractionate during differentiation of the lavas after emplacement (Appendix 1).

The evolution of Cr concentrations during differentiation of the komatiite lavas is shown in Figure 1. The data fall within the same general evolution trend of Cr concentrations presented in Figure 1 (modified from Arndt et al 2008). Olivine is the liquidus phase in komatiites and its crystallisation

reduces the Mg content of the melt. Figure 1 shows that during early crystallisation, where olivine is the only phase crystallising, there is a slight increase in the Cr concentration of the residual melt. Chromium concentrations increase until the melt becomes saturated in Cr, and chromite starts to crystallize. Once chromite starts crystallising, the Cr content of the residual melt decreases. This general trend is shown in the combined komatiite data, however, there are differences between the individual lava flows. In the following, the discussion is focused on Tony's Flow and Victoria's Lava Lake, as the samples from Gorgona may represent multiple flows, making trends from this locality less pronounced. There are two main differences between the Victoria's Lava Lake and Tony's Flow with respect to behaviour of Cr; (1) The Victoria's Lava Lake does not show an increase in Cr concentrations in it's high MgO samples and (2) the Cr saturation lines of the two flows are offset.

Chromite begins to crystallise once a lava is saturated in Cr. Chromium is less soluble under more oxidising conditions and lower Mg (Barnes, 1998; Murck and Campbell, 1986). During olivine fractionation, the Mg content of a komatiite magma decreases leading to Cr saturation. Once saturation is reached the composition of the magma will evolve along the Cr saturation curve. The saturation curves presented in Figure 4 are fitted to the composition of the komatiites in this study. The Victoria's Lava Lake does not show an increase in the Cr concentration in the first komatiites to crystallise (Figure 2b). Therefore, the flow had already reached saturation in Cr in the emplaced lava when crystallisation began, and chromite and olivine co-precipitated over the entire range of compositions. The fact that chromite crystallisation was not delayed in this system, could explain the lower Cr content of the olivine.

The position of the chromite saturation curve in the MgO vs Cr space will be controlled by the oxidation state of Cr. Figure 4 shows that chromite saturation is suppressed in Tony's Flow compared to the Victoria's Lava Lake. This can be explained by higher $Cr^{2+}/\Sigma Cr_{TOT}$ in Tony's Flow. The $Cr^{2+}/\Sigma Cr_{TOT}$ is controlled by the oxygen fugacity of the lava, the temperature and composition (Hanson and Jones,

1998; Li et al., 1995; O'Neill and Berry, 2006; Sossi and O'Neill, 2016). The oxygen fugacities of Tony's Flow and the Victoria's Lava Lake are indistinguishable, ΔFMQ= +0.48 ± 0.27 and ΔFMQ = +0.43 ± 0.26, respectively (Nicklas et al., 2016, 2018). Therefore, the difference in $Cr^{2+}/\Sigma Cr_{TOT}$ must arise from Tony's Flow having a higher liquidus temperature and a different composition compared to Victoria's Lava Lake (Puchtel et al., 2016, 2009).

To summarise, the different Cr behaviour in Tony's Flow and Victoria's Lava Lake can be explained by the differences in the Mg content of their emplaced lavas and their liquidus temperatures. The lower Mg content of the Victoria's Lava Lake means that chromite and olivine co-crystallised over the entire range of the lava lake compositions. Higher temperatures and a different composition for Tony's Flow with respect to the Victoria's Lava Lake increased the $Cr^{2+}/\Sigma Cr_{TOT}$ ratio and the Cr saturation limit (Figure 4).

The Gorgona komatiites do not show clear trends, unlike the other two komatiite systems studied here (Figure 2). There is a decrease in the Cr content with decreasing Mg abundances in these komatiites. Major element variations indicate that the major liquidus minerals in these komatiite were also olivine and chromite. Although it is not possible to tell when chromite crystallisation began, the Gorgona komatiites behave similarly to other komatiites, as shown by them plotting within MgO-Cr space of other komatiites (Figure 1). Variations in both [Cr] and $\delta^{53}Cr$ suggest that the Gorgona komatiites have evolved most closely to Tony's Flow.

5.2. Non-magmatic effects on the $\delta^{53}Cr$ of komatiites

In order to ascertain the manner in which Cr isotopes were fractionated during crystallisation, it is first necessary to assess the effect of non-magmatic processes on $\delta^{53}Cr$. The older komatiites analysed in this study are described as remarkably fresh (Nisbet et al., 1987; Puchtel et al., 1996; Renner

et al., 1994). However, this is relative to rocks that are billions of years old. Common alteration of Archean komatiites included serpentinisation, which has been identified as a process that can affect Cr stable isotopes (Farkaš et al., 2013). Although many of the komatiites in this study preserved most of their primary olivine, there are parts of the komatiite flows that experienced partial replacement of olivine by serpentine. Weathering is a low temperature process that can affect the δ^{53}Cr of rocks (Frei et al., 2014). Additionally, the ascent of komatiite magmas to the surface can result in entrainment of crustal material, which was shown to have modified the composition of the primary magma (Puchtel et al., 2016). Therefore, before the effects of fractional crystallisation are considered in more detail, the extent to which these non-magmatic processes have overprinted the Cr isotope composition must be assessed.

5.2.1. Crustal Contamination

The extent of crustal contamination in the komatiites from this study has previously been evaluated using the lithophile trace element systematics. The Victoria's Lava Lake was calculated to have experienced ~4% assimilation of tonalite material (Puchtel et al., 2016). The trace element compositions of Tony's Flow and the Gorgona komatiites show no evidence of significant crustal contamination (Puchtel et al., 2009; Révillon et al., 2002).

The δ^{53}Cr compositions of crustal material has a large range due to the greater magnitude of fractionations that occur at low temperatures and during melt fractionation (e.g., Bonnand et al., 2013; Frei et al., 2014). Mixing with such material could in principle change the δ^{53}Cr of the primary komatiite magma. However, the tonalite material that mixed with the Victoria's Lava Lake samples contains much less Cr than komatiites (40 μg g^{-1} compared to 2000 μg g^{-1} (Puchtel et al., 2016)), so the contribution to the Cr budget of komatiites from crustal material will be < 0.1 %. In order for crustal assimilation to have an effect on the δ^{53}Cr Victoria's Lava Lake komatiite system, outside of the analytical uncertainty of

our measurements, the contaminant must have had δ^{53}Cr value of >20 ‰. So far, no natural terrestrial samples are known to have δ^{53}Cr compositions even approaching this value.

5.2.2. Chemical Alteration

The old age of komatiites means that they may have been exposed to many post-magmatic processes that could have altered their chemical composition. One method to identify if an element was immobile is to demonstrate that it lies along an olivine control line (Arndt, 1994). Application of this tool is not as straightforward for Cr, as the crystallisation of chromite can also affect the liquid evolution line. However, there are well known trends for Cr evolution in komatiite lava flows (Murck and Campbell, 1986), which the samples in this study closely adhere to (Figure 2a), showing that Cr was not mobilized in these komatiites. This is in agreement with previous studies that the Cr contents of the komatiite flows utilised in this study have not been modified by alteration (Kerr et al., 1996; Puchtel et al., 2016, 2009).

Another process that may have altered the δ^{53}Cr composition of komatiites is weathering (Frei et al., 2014) and post eruptional hydration. These authors showed that removal of more soluble and isotopically heavy Cr^{6+} results in the weathered rocks becoming isotopically lighter. Two methods were used here to investigate the effects of weathering, the mafic index of alteration (MIA) and the chemical index of alteration (CIA). The MIA uses the molar ratio of mobile elements to mobile and immobile elements (Equation 1 and 2) (Babechuk et al., 2014). Different expressions can be used to account for the behaviour of Fe in oxidising and reducing environments.

Eq(1) $$MIA[r] = 100 \times \left[Al_2O_3 / \left(Al_2O_3 + Fe_2O_{3(T)} + MgO + CaO + Na_2O + K_2O \right) \right]$$

Eq(2) $$MIA[o] = 100 \times \left[(Al_2O_3 + Fe_2O_{3(T)}) / \left(Al_2O_3 + Fe_2O_{3(T)} + MgO + CaO + Na_2O + K_2O \right) \right]$$

Eq(3) $CIA = 100 \times [Al_2O_3/(Al_2O_3 + CaO + Na_2O + K_2O)\,]$

Due to the lower atmospheric oxygen concentrations in the Precambrian, the MIA[r] may be the best choice for the Victoria's Lava Lake and Tony's Flow. However, the choice of the index does not affect the result, as neither shows any correlation with $\delta^{53}Cr$ (Figure 5a and 5b). The CIA is an alternative index that does not include mafic elements (MgO and $Fe_2O_{3(T)}$) in the calculation (Nesbitt and Young, 1984, 1982). There is no correlation between the CIA and $\delta^{53}Cr$ either (Figure 5c). It should also be noted that the range in the CIA values for the komatiites is very small, showing that these flows have not been significantly chemically altered in terms of Cr isotopic composition.

Victoria's Lava Lake and Tony's Flow. However, the choice of the index does not affect the result, as neither shows any correlation with $\delta^{53}Cr$ (Figure 5a and 5b). Furthermore, there is no correlation between the CIA and $\delta^{53}Cr$ (Figure 5c). It should also be noted that the range in the CIA values for the komatiites is very small, showing that these flows have not been extensively altered.

5.2.3. Serpentinisation

Serpentinisation is a common alteration process in komatiites, during which olivine and other minerals react with high-temperature fluids. Samples from Tony's Flow and the Victoria's Lava Lake were selected which show limited evidence of this alteration (Nisbet et al., 1987; Puchtel et al., 1996). Farkaš *et al.*, (2013) has shown that serpentinisation can lead to an increase in $\delta^{53}Cr$. The loss on ignition (LOI) index is used to quantify the amount of serpentinisation that has occurred in the three komatiite systems. No systematic variations between LOI and $\delta^{53}Cr$ are seen for the samples from this study (Figure 6).

It is clear that the $\delta^{53}Cr$ of the studied komatiites has not been affected by contamination or post-magmatic processes, and, as such, the variations within the flows are explained solely in terms of magmatic processes in the following sections.

5.3. Magmatic Cr isotope fractionation within komatiite flows

Magmatic processes have previously been shown to fractionate Cr isotope compositions. The $\delta^{53}Cr$ value of basalts can be slightly lighter than that of the BSE (Schoenberg et al., 2008; Shen et al., 2019; Xia et al., 2017), suggesting that melting or differentiation produces magmas that are isotopically lighter. At higher degrees of melting, applicable to the formation of komatiites, Rayleigh fractional melting models suggest that the composition of melts will become closer to that of the mantle. However, Shen et al (2018) created non-modal melting models to explore the effects of melting on the fractionation factor and concluded that greater $\Delta^{53}Cr_{mantle\text{-}melt}$ existed at 10 % partial melting compared to 1 % partial melting. This result was not seen in later work on basaltic suites found the opposite, that larger $\Delta^{53}Cr_{mantle\text{-}melt}$ occurred during the formation of lower degree melts compared to higher degree

melts (Bonnand et al., 2020). Komatiites formed under different mantle conditions compared to basalts under which Cr and Cr isotopes behave differently.

Previous studies of komatiites show that there is no detectable differences between the average Cr isotope composition of komatiites and that of mantle peridotites (Sossi et al., 2018), suggesting that there is no Cr isotope fractionation during their formation. This is expected when the greater fraction of Cr komatiites contains and smaller fractionation factors at higher temperatures are considered. The conditions that komatiite form reduces the compatibility of Cr (Appendix 1). Briefly, melting a source that contains garnet and the higher temperatures decreases the compatibility of Cr in the mantle. The higher degree of melting also leads to a higher fraction of the initial Cr entering the liquid phase (Figure A.2.). These effects are shown using non-modal melting models (Sossi and O'Neill, 2017). In order to balance the Cr in the system, the δ^{53}Cr difference between the melt and the mantle will decrease as a greater faction of Cr is removed from the mantle.

Higher temperature melting decreases equilibrium isotope fractionation factors through the relationship $\Delta^{53}Cr_{mantle\text{-}melt} \propto 1/T^2$ (Schauble, 2004). The greater temperature of komatiite formation (Arndt et al., 1997) compared to basalts will lead to half $\Delta^{53}Cr_{mantle\text{-}melt}$. On the basis of these observations the composition of the primary komatiite melt is expected to be within error of the mantle sources from which they formed.

Fractional crystallisation can also affect the δ^{53}Cr of magmas, with basaltic suites becoming isotopically lighter at more evolved compositions (Bonnand et al., 2020, 2016a; Shen et al., 2019). The stable Cr isotope composition is heavier in the more evolved samples from Tony's Flow and Gorgona, while the Victoria's Lava Lake komatiites do not show any variation (Figure 2a). The trend between MgO and δ^{53}Cr of the Tony's Flow komatiites is clearest in the more evolved samples, while there is a greater

scatter at higher MgO contents. The variation in $\delta^{53}Cr$ of these flows requires fractional crystallisation of an isotopically light phase.

Theoretical considerations of equilibrium isotopic fractionation suggest that olivine will be isotopically lighter than the melt and other phases in komatiites. Light isotopes are preferentially included in minerals that have lower oxidation states, and higher mineral coordination numbers (Schauble, 2004). The two minerals that host Cr within komatiites are olivine and chromite. Olivine contains Cr within octahedral sites (C.N. = 6) and can contain both Cr^{2+} and Cr^{3+}. Spinel also hosts Cr in octahedral sites (apart from pure end members which can also contain Cr in tetrahedral sites, C.N. = 4), but only contains Cr^{3+} (Roeder and Reynolds, 1991). Therefore, olivine is expected to be the isotopically lighter phase. Theoretical calculations and analysis of mineral separates agree that olivine is isotopically lighter compared to Cr-oxides (Shen et al., 2018, 2016) and the melt from which they formed (Shen et al., 2019). Fractionation of isotopically lighter olivine is a plausible explanation for the $\delta^{53}Cr$ variations in the komatiites. Samples with high Mg contents and light $\delta^{53}Cr$ likely formed by the addition of olivines, while low Mg and high $\delta^{53}Cr$ komatiites are residual melts formed following the removal of isotopically lighter olivine.

The evolution of Tony's Flow can be modelled using fractional crystallisation equations (Shaw, 1970), in order to estimate the $\Delta^{53}Cr_{olivine\text{-}melt}$. Initially the only mineral crystallising is olivine, therefore $\Delta^{53}Cr_{solid\text{-}melt} = \Delta^{53}Cr_{olivine\text{-}melt}$. At lower Mg concentrations (< 21 % MgO), chromite begins to crystallise as well. It is assumed that chromite is forming with a composition similar to the melt ($\Delta^{53}Cr_{solid\text{-}melt} \approx 0$), therefore, the $\Delta^{53}Cr_{solid\text{-}melt}$ can be given by the ratio of Cr in olivine to chromite. Komatiites which have higher Mg contents than the initial melt are formed through the accumulation of olivine with a constant isotopic composition. It should be noted that while olivine accumulation leads to progressively isotopically lighter cumulates, this reflects the use of a constant isotopic composition. In reality, the

isotopic composition of the olivine will become heavier as the differentiating parent melt becomes more evolved and heavier. Therefore, the change in $\delta^{53}Cr$ of cumulate komatiites with higher Mg as shown in Figure 7 can be assumed to be a lower limit.

The model is presented in Figure 7. In order to recreate the variations seen $\Delta^{53}Cr_{olivine\text{-}melt}$ = -0.2‰ is required. This value is nearly twice that of previous estimates (Shen et al., 2019). This is most likely caused by differences in the behaviour of Cr in komatiite melts compared to other silicate melts. The sites available to Cr are determined by the composition of the melt; Mg and Si ions tend to form tetrahedral sites (O'Neill and Berry 2006) which can contain Cr^{2+}, whereas Ca, among other cations, form octahedral sites, which contain Cr^{3+}. The composition of komatiitic melts results in a high tetrahedral to octahedral site ratios, which leads to stabilisation of Cr^{2+} in melts (Miletich et al., 1999 O'Neill and Berry 2006). The stabilisation of Cr^{2+} in high Mg melts (O'Neill and Berry 2006) may make these sites more energetically favourable for Cr ions. This change in the zero-point energy of the site will lead to isotopically heavy Cr^{2+} in the melt compared to Cr^{2+} in solid phases. This effect will be greatest for komatiites crystallising from high Mg, low Ca melts, such as Tony's Flow and Gorgona, compared to Victoria's Lava Lake.

The Victoria's Lava Lake has the same mineralogy as other komatiite flows, therefore, the same Cr isotope trends may be expected in this system. However, no $\delta^{53}Cr$ variations are seen (Figure 2a). The $\delta^{53}Cr$ composition of chromites from Victoria's Lava Lake komatiites have the same $\delta^{53}Cr$ composition as the bulk rocks (Figure 3), which suggests that the $\delta^{53}Cr$ in the Victoria's Lava Lake komatiites are determined by chromite. In other komatiites, Cr is distributed more evenly between olivine and chromites. However, in the Victoria's Lava Lake, olivine has lower Cr concentrations, (565-806 µg g^{-1}, Puchtel *et al.*, 2016). The low Cr concentrations of olivine in this flow is likely due to a lower $Cr^{2+}/\Sigma Cr_{TOT}$ (Figure 4). This (i) decreases the compatibility of chromium in the melt and, therefore, chromite

crystallisation is not delayed and (ii) reduces the availability of Cr^{2+} to enter olivine crystal lattice (Donaldson, 1982; Shore, 1996). The lower Mg content of the Victoria's Lava Lake komatiites results in a lower abundance of olivine compared to other komatiite flows, further reducing the fraction of Cr hosted in olivine compared to other flows. The amount of Cr contained in olivine is no more than 7 % of the total Cr budget (Table A.1). Assuming a similar fractionation between olivine and melt in this flow as that calculated for Tony's flow ($\Delta^{53}Cr_{olivine\text{-}melt}$ = -0.20 ‰), the Cr isotope composition of the Victoria's Lava Lake bulk rocks will closely match that of the chromite.

5.4. Differences in δ^{53}Cr isotope fractionation during crystallisation between komatiitic and other magmas

Previous studies have investigated δ^{53}Cr isotope fractionation during crystallisation of lunar and terrestrial basalts (Bonnand et al., 2020, 2016a; Shen et al., 2019). All these studies found that during crystallisation, melts became progressively lighter in δ^{53}Cr, although $\Delta^{53}Cr_{solid\text{-}melt}$ varies between suites. Crystallisation of lunar basalts shows the greatest variation in δ^{53}Cr (Bonnand et al., 2016a). The δ^{53}Cr variation is explained by the crystallisation of isotopically heavy spinel which leads to the melt becoming progressively lighter. The difference in δ^{53}Cr across the suite is greater for lunar basalts compared to basaltic suites from Hawai'i and Fangataufa (Bonnand et al., 2020; Shen et al., 2019), which is explained by the crystallisation of pyroxene along with spinel. The lighter isotopic composition of pyroxene limits the $\Delta^{53}Cr_{solid\text{-}melt}$ and reduces the amount of fractionation that occurs. The δ^{53}Cr variations are greatest at the end of the sequence of crystallisation as the liquid they form from becomes highly fractionated.

The komatiites show different behaviour, with isotopically light olivine leading to increasingly heavier δ^{53}Cr. The contrasting isotopic evolution displayed in this study can be understood in terms of the redox conditions, temperature, and magma compositions (Figure A.3). Lunar basalts and terrestrial basalts have different $Cr^{2+}/\Sigma Cr_{TOT}$, explained by different redox conditions and temperature (Berry et al.,

2006; Li et al., 1995). The komatiite samples have higher $Cr^{2+}/\Sigma Cr_{TOT}$ ratios despite forming at similar fO_2 values to terrestrial basalts. Komatiites form from higher temperature magmas which will increase the $Cr^{2+}/\Sigma Cr_{TOT}$, however the different behaviour is also due to the composition. The $Cr^{2+}/\Sigma Cr_{TOT}$ ratio can vary greatly for different compositions, and is sensitive to changes in the Ca and Mg concentrations (Berry et al 2006). The lower Ca and higher Mg of komatiitic melts means there are fewer octahedral and more tetrahedral sites, which stabilises Cr^{2+} in the melt and may lead to more energetically favourable mineral sites (Miletich et al., 1999; O'Neill and Berry, 2006). The higher $Cr^{2+}/\Sigma Cr_{TOT}$ ratio in the lunar basalts is due to lower fO_2, and not differences to the sites that Cr occupies in the melt, therefore, Cr^{2+} in lunar melts will not have been energetically favourable compared to terrestrial basalts, and so crystallisation of Cr^{2+} bearing minerals will not be isotopically light.

5.5. Estimates of Cr isotopic composition of the BSE

The $\delta^{53}Cr$ BSE composition can be estimated using the initial composition of komatiite melts. No fractionation occurs during the formation of the komatiite melts; therefore, the Cr composition of the initial melt will reflect that of the source mantle. Komatiites have the advantage over mantle peridotites in that small-scale $\delta^{53}Cr$ variations in the source are homogenized as a much larger volume of the mantle is sampled. Therefore, the small-scale effects of metasomatism, which lead to increases in the uncertainties in estimates for the BSE using mantle peridotites, are removed. The choice of method to calculate the $\delta^{53}Cr$ of the initial melts is discussed in order to provide a well-constrained and robust BSE estimate.

In Sossi et al. (2018), the komatiite samples used in their calculation of the $\delta^{53}Cr$ BSE composition were those with A_1 and A_2 spinifex textures. Although composition of these samples is

considered to be close to the initial composition of the komatiite melt (Faure et al., 2006; Sossi et al., 2018), A1 and A2 spinifex-textured komatiites do show variations in the Mg and Cr concentrations within individual komatiite lava flows (Table 1). Even these early formed parts of komatiite flows have experienced some degree of fractional crystallisation, which may cause variations in the δ^{53}Cr isotope composition, as seen by the spread of δ^{53}Cr compositions (Figure 8.). An average composition of spinifex-textured A1 and A2 komatiites from this study and Sossi et al. (2018) is -0.12 ± 0.06 ‰ (2 s.d., n =26), with the relatively large uncertainty on the average reflecting the above effect.

Two other methods for estimating the Cr isotopic composition of the BSE are presented here. Komatiite samples analysed in this study, have been combined with selected samples from Sossi et al. (2018), in the calculations. In order to ensure that representative values of the initial melt are given for each location, only flows with multiple samples were used. Two komatiite flows from Sossi et al. (2018), namely, Munro and Komati, both of which had 3 or more komatiite samples analysed, met these requirements. One sample (49J) from the Komati flow was left out of the calculation as it appears to have crystallised from a different parental melt.

The first alternative approach is to use komatiites with chemical compositions closest to that of the initial melt rather than using the textures of komatiites to identify the best samples. The MgO content of the melt can be estimated by calculating the composition that the most MgO-rich olivine would be in equilibrium with (e.g. Bickle, 1982; Nisbet et al., 1993; Toplis, 2005). The komatiite sample with the MgO content closest to this initial value is assumed to be representative of the initial melt (e.g. Hibbert et al., 2012). The initial melt MgO contents were taken from literature sources (Arndt et al., 1997; Puchtel et al., 2016, 2009; Sossi et al., 2016) and the komatiite from each flow with the closest composition were selected as the best representation of the melt (Table 2). The average δ^{53}Cr of these komatiite samples returns a BSE value of -0.13 ± 0.07 ‰ (n =5). However, this method selects some

δ^{53}Cr komatiite values that are at the light end of the δ^{53}Cr range of values within komatiite flows (e.g., for Komati, Munro and Tony's Flow, Table 2). This suggests that samples with the MgO content of the initial flow do not always represent quenched komatiites. Instead, the MgO content could be the result of a combination of olivine accumulation and fractional crystallisation, which will not provide the δ^{53}Cr composition of the initial melt.

The second approach is to use a weighted average of the compositional variability within a flow by summing all parts measured. While komatiite flows have differentiated, this occurred after the lava flows were emplaced, therefore summing all parts of the flow will recreate the initial liquid composition. A weighted average must be used as the large range in Cr concentrations varies with the δ^{53}Cr of the komatiites (Figure 8). Carrying out the calculations this way requires that the flow is equally sampled. This can be checked by taking the average Mg or Cr concentrations of the komatiite flows and comparing them to the initial melt composition. For all flows in this study, the average Mg content is within 15% of that of the initial melt, showing that the sampling recreates the composition of the initial melt. The same is true for flows for which initial Cr concentration data is available, with recreated values within 10%. The Victoria's Lava Lake komatiites represent a fractionated melt, however, we assume that this, like the later crystallisation, did not lead to any isotope variations. While this method is unable to entirely sample the flows, the close agreement in δ^{53}Cr between the flows with better coverage (i.e. Victoria's Lava Lake and Tony's Flow) and those with fewer samples, along with the close match to the recreated initial composition, provides evidence that the results are robust. The weighted averages of the flows are presented in Table 2. The average Cr isotopic composition of the initial komatiite melts is -0.12 ± 0.04 ‰ (n = 5).

It is worth noting that the initial δ^{53}Cr composition is reproduced across the flows. Some variations may be expected due to the different conditions of melting, initial mantle compositions or

sections of the flow not included in the average, however, this is not observed. This confirms the robustness of using komatiite flows versus other samples, as well as using the weighted average to estimate the $\delta^{53}Cr$ of the initial komatiite melt.

On this basis, a more precise value of -0.12 ± 0.04 ‰ of the BSE composition is proposed. This value is in agreement with the previous estimates calculated using peridotites ($\delta^{53}Cr$ =-0.12 ± 0.10 ‰ (Schoenberg et al., 2008), -0.14 ± 0.12 (Xia et al., 2017) and $\delta^{53}Cr$ = -0.11 ± 0.06 ‰ (Sossi et al., 2018)).

The new BSE composition can be used to re-evaluate deviations between previously measured samples and the BSE using a two-tailed Student's t test. There was no significant difference with the compositions of ordinary chondrites or carbonaceous chondrites, which agrees that there was no Cr isotopic fractionation during core formation (Bonnand et al., 2016b; Schoenberg et al., 2016). There are insufficient enstatite chondrite data to compare. There is a statistical significant difference between the $\delta^{53}Cr$ composition of the BSE and that of the HED, which agrees with Zhu et al. (2019) that there has been loss of heavy Cr isotopes during formation of Vesta.

Basaltic suites were also analysed using a two-tailed Student's t test (Bonnand et al., 2020; Shen et al., 2019). Five different suites were analysed, with 4 having a resolvable difference in isotopic composition. The Kilauea Iki suite (Shen et al., 2019), which did not have a resolvable difference from the mantle, has the highest MgO wt%., suggesting that it represents a higher degree of melting. Therefore, resolvable isotopic shifts can only occur during low degree partial melting of the mantle.

The weighted average composition of komatiites shows that there has not been a change in the Cr isotope composition in the mantle over the past 3.5 Ga (Figure 9). Melting in the modern mantle is able to produce small fractionations during melting (Bonnand et al., 2020; Shen et al., 2019), however the small differences between melt and mantle and the fraction of Cr removed is not large enough to

change the isotopic composition of the mantle. In the past, the behaviour of Cr during mantle melting would have been different, with higher temperatures reducing equilibrium fractionation, as well as increasing the amount of Cr in partial melts. Overall, this would have led to even smaller Cr isotope fractionations and the δ^{53}Cr composition of the mantle would not be expected to change through time. This is illustated by the consistent composition of komatiites (Figure 9).

6. Conclusions

The δ^{53}Cr values from komatiites from three komatiite systems ranging in age from 2.7 Ga to 89 Ma, have been collected using high precision techniques. Komatiites from three systems, ranging in age from 2.7 Ga to 89 Ma, show resolvable δ^{53}Cr variations within individual lava flows, and variable [Cr] and δ^{53}Cr behaviour between flows.

Chromium isotope and concentration variations in komatiites were controlled by fractional crystallisation of chromite and olivine, and the conditions under which these minerals form. The 2.4 Ga Victoria's Lava Lake samples reflect crystallisation of chromite and olivine throughout the sequence, whereas the 2.7 Ga Tony's Flow had a period of olivine-only crystallisation prior to Cr saturation in the residual melt. A systematic difference between the saturation of chromite in these two flows is due to the higher temperatures, different compositions, and, therefore, higher $Cr^{2+}/\Sigma Cr_{TOT}$ in Tony's Flow.

The Cr isotope composition variations within Tony's Flow and Gorgona komatiites are explained by different amounts of isotopically lighter olivine distributed throughout the lavas. A plausible difference between the melt and olivine of -0.20 ‰ can reproduce 0.10 ‰ variations within the Tony's Flow komatiites. No isotope variation is seen within the Victoria's Lava Lake. This is explained by the lower Cr concentrations in olivine, due to the co-crystallisation of olivine and chromite throughout this unit.

Using the komatiite $\delta^{53}Cr$ data from this study and previous work has enabled us to obtain a new estimate for the Cr isotopic composition of the BSE. Past methods for calculating the stable Cr isotope composition of komatiites, such as only considering spinifex-textured komatiites, or using komatiites with chemical compositions that are closest to the emplaced lava composition, gave less precise estimates. A weighted average of five komatiite flows provides a better constrained value of $\delta^{53}Cr$ -0.12 ± 0.04 ‰. The agreement between the Cr isotopic composition of the BSE obtained using komatiites and those obtained using other methods provide additional evidence that melting does not lead to significant changes in $\delta^{53}Cr$.

Declaration of Competing Interests

The authors declare that they have no known competing financial interests or personal relationships that could have appeared to influence the work reported in this paper.

Acknowledgments

Research funding for this work was provided by the Science and Technology Facilities Council (STFC) to A.N.H. (STFC Planetary Origins and Developments: ST/M001318/1). ISP acknowledges support from the NSF EAR-1754186. We thank Phil Holdship and Alan Hsieh for providing instrumental support, and to Steve Wyatt and Jane Barling for laboratory support. We would like to P. Sossi and one anonymous reviewers for their useful comments that helped to improve the manuscript. Data supporting the publication can be accessed by contacting MJ.

7. References

Armytage, R.M.G., Georg, R.B., Savage, P.S., Williams, H.M., Halliday, A.N., 2011. Silicon isotopes in meteorites and planetary core formation. Geochim. Cosmochim. Acta 75, 3662–3676. https://doi.org/10.1016/j.gca.2011.03.044

Arndt, N. T, Kerr, A.C., Arndt, Nicholas T, Kerr, A.C., Tarney, J., 1997. Dynamic melting in plume heads : The formation of Gorgona komatiites and basalts Dynamic melting in plume heads : the formation of Gorgona komatiites and basalts. Earth Planet. Sci. Lett. 146, 289–301. https://doi.org/10.1016/S0012-821X(96)00219-1

Arndt, N.T., 2008. Komatiite. Cambridge University Press.

Arndt, N.T., 1994. Archean Komatiites, in: Condie, K.C. (Ed.), Archean Crustal Evolution. Elsevier, pp. 11–44.

Arndt, N.T., Ginibre, C., Chauvel, C., Albarède, F., Cheadle, M.J., Herzberg, C., Jenner, G., Lahaye, Y., 1998. Were komatiites wet? Geology 26, 739–742. https://doi.org/10.1130/0091-7613(1998)026<0739:WKW>2.3.CO;2

Arndt, N.T., Nisbet, E.G., 1982. What is a komatiite?, in: Arndt, N.T., Nisbet, E.G. (Eds.), Komatiites. George Allen and Unwin, London, pp. 19–28.

Babechuk, M.G., Widdowson, M., Kamber, B.S., 2014. Quantifying chemical weathering intensity and trace element release from two contrasting basalt profiles, Deccan Traps, India. Chem. Geol. 363, 56–75. https://doi.org/10.1016/j.chemgeo.2013.10.027

Badullovich, N., Moynier, F., Creech, J., Teng, F.-Z., Sossi, P.A., 2017. Tin isotopic fractionation during igneous differentiation and Earth's mantle composition. Geochemical Perspect. Lett. 24–28. https://doi.org/10.7185/geochemlet.1741

Barnes, S.J., 1998. Chromite in Komatiites, 1. Magamatic Controls on Crystallization and Composition. J. Petrol. 39, 1689–1720. https://doi.org/10.1093/petroj/39.10.1689

Berry, A.J., O'Neill, H.S.C., Scott, D.R., Foran, G.J., Shelley, J.M.G., 2006. The effect of composition on Cr 2 + / Cr 3 + in silicate melts. Am. Mineral. 91, 1901–1908. https://doi.org/10.2138/am.2006.2097

Bickle, M.J., 1982. The magnesium contents of komatiitic liquids, in: Arndt, N.T., Nisbet, E.G. (Eds.), Komatiites. George Allen and Unwin, London, pp. 479–494.

Bickle, M.J., Martin, A., Nisbet, E.G., 1975. Basaltic and peridotitic komatiites and stromatolites above a basal unconformity in the Belingwe greenstone belt, Rhodesia. Earth Planet. Sci. Lett. 27, 155–162. https://doi.org/10.1016/0012-821X(75)90024-2

Bonnand, P., Doucelance, R., Boyet, M., Bachèlery, P., Bosq, C., Auclair, D., Schiano, P., 2020. The influence of igneous processes on the chromium isotopic compositions of terrestrial basalts. Earth Planet. Sci. Lett. 532, 116028. https://doi.org/10.1016/j.epsl.2019.116028

Bonnand, P., Halliday, A.N., 2018. Oxidized conditions in iron meteorite parent bodies. Nat. Geosci. 11, 2–6. https://doi.org/10.1038/s41561-018-0128-2

Bonnand, P., James, R.H., Parkinson, I.J., Connelly, D.P., Fairchild, I.J., 2013. The chromium isotopic composition of seawater and marine carbonates. Earth Planet. Sci. Lett. 382, 10–20. https://doi.org/10.1016/j.epsl.2013.09.001

Bonnand, P., Parkinson, I.J., Anand, M., 2016a. Mass dependent fractionation of stable chromium isotopes in mare basalts: Implications for the formation and the differentiation of the Moon. Geochim. Cosmochim. Acta 175, 208–221. https://doi.org/10.1016/j.gca.2015.11.041

Bonnand, P., Williams, H.M., Parkinson, I.J., Wood, B.J., Halliday, A.N., 2016b. Stable chromium isotopic composition of meteorites and metal-silicate experiments: Implications for fractionation during core formation. Earth Planet. Sci. Lett. 435, 14–21. https://doi.org/10.1016/j.epsl.2015.11.026

Chauvel, C., Dupré, B., Arndt, N.T., 1993. Pd and Nd isotopic correlation in Belingwe komatiites and basalts, in: The Geology of the Belingwe Greenstone Belt, Zimbabwe. A Study of the Evolution of Archean Continental Crust. A.A. Balkema, Rotterdam/Brookfield. pp. 205–220.

Dauphas, N., Teng, F.Z., Arndt, N.T., 2010. Magnesium and iron isotopes in 2.7 Ga Alexo komatiites: Mantle signatures, no evidence for Soret diffusion, and identification of diffusive transport in zoned olivine. Geochim. Cosmochim. Acta 74, 3274–3291. https://doi.org/10.1016/j.gca.2010.02.031

Donaldson, C.H., 1982. Spinifex-textured komatiites: a review of textures, compositions and layering, in: Arndt, N.T., Nisbet, E.G. (Eds.), Komatiites. George Allen and Unwin, pp. 211–244.

Echeverria, L.M., 1980. Mineralogy and Petrology Tertiary or Mesozoic Komatiites From Gorgona Island , Colombia : Field Relations and Geochemistry. Contrib. to Mineral. Petrol. 266, 253–266.

Ellis, A.S., Johnson, T.M., Bullen, T.D., 2002. Chromium Isotopes and the Fate of Hexavalent Chromium in the Environment. Science (80-.). 295, 2060–2062.

Farkaš, J., Chrastný, V., Novák, M., Čadkova, E., Pašava, J., Chakrabarti, R., Jacobsen, S.B., Ackerman, L., Bullen, T.D., 2013. Chromium isotope variations (??53/52Cr) in mantle-derived sources and their weathering products: Implications for environmental studies and the evolution of ??53/52Cr in the Earth's mantle over geologic time. Geochim. Cosmochim. Acta 123, 74–92. https://doi.org/10.1016/j.gca.2013.08.016

Faure, F., Arndt, N.I., Libourel, G., 2006. Formation of spinifex texture in komatiites: An experimental study. J. Petrol. 47, 1591–1610. https://doi.org/10.1093/petrology/egl021

Fischer, R.A., Nakajima, Y., Campbell, A.J., Frost, D.J., Harries, D., Langenhorst, F., Miyajima, N., Pollok, K., Rubie, D.C., 2015. High pressure metal-silicate partitioning of Ni, Co, V, Si and O. Geochim. Cosmochim. Acta 167, 177–194. https://doi.org/10.1016/j.gca.2015.06.026

Frei, R., Poiré, D., Frei, K.M., 2014. Weathering on land and transport of chromium to the ocean in a subtropical region (Misiones, NW Argentina): A chromium stable isotope perspective. Chem. Geol. 381, 110–124. https://doi.org/10.1016/j.chemgeo.2014.05.015

Gall, L., Williams, H.M., Halliday, A.N., Kerr, A.C., 2017. Nickel isotopic composition of the mantle. Geochim. Cosmochim. Acta 199, 196–209. https://doi.org/10.1016/j.gca.2016.11.016

Gansser, A., Dietrich, V.J., Cameron, W.E., 1979. Palaeogene komatiites from Gorgona Island. Nature 278, 1978–1979.

Greber, N.D., Puchtel, I.S., Nägler, T.F., Mezger, K., 2015. Komatiites constrain molybdenum isotope composition of the Earth's mantle. Earth Planet. Sci. Lett. 421, 129–138. https://doi.org/10.1016/j.epsl.2015.03.051

Green, D.H., 1975. Genesis of archean peridotitic magmas and constraints on archean geothermal gradients and tectonics. Geology 3, 15–18. https://doi.org/10.1130/0091-7613(1975)3<15:GOAPMA>2.0.CO;2

Hanson, B., Jones, J.H., 1998. The systematics of Cr3+ and Cr2+ partitioning between olivine and liquid in the presence of spinel. Am. Mineral. 83, 669–684.

Hibbert, K.E.J., Williams, H.M., Kerr, A.C., Puchtel, I.S., 2012. Iron isotopes in ancient and modern komatiites: Evidence in support of an oxidised mantle from Archean to present. Earth Planet. Sci. Lett. 321–322, 198–207. https://doi.org/10.1016/j.epsl.2012.01.011

Hunter, M.A., Bickle, M.J., Nisbet, E.G., Martin, A., Chapman, H.J., 1998. Continental extensional setting for the Archean Belingwe Greenstone Belt, Zimbabwe. Geology 26, 883–886. https://doi.org/10.1130/0091-7613(1998)026<0883:CESFTA>2.3.CO;2

Kerr, A.C., 2005. La Isla de Gorgona, Colombia: A petrological enigma? Lithos 84, 77–101. https://doi.org/10.1016/j.lithos.2005.02.006

Kerr, A.C., Marriner, G.F., Arndt, N.T., Tarney, J., Nivia, A., Saunders, A.D., Duncans, R.A., 1996. The petrogenesis of Gorgona komatiites, picrites and basalts: new field, petrographic and geochemical constraints. Lithos 37, 245–260.

Kulikov, V.S., Bychkova, Y. V., Kulikova, V., Ernst, R., 2010. The Vetreny Poyas (Windy Belt) subprovince of southeastern Fennoscandia: An essential component of the ca. 2.5-2.4Ga Sumian large igneous provinces. Precambrian Res. 183, 589–601. https://doi.org/10.1016/j.precamres.2010.07.011

Kushiro, I., Yoder, H.S., 1969. No Title. Carangie Inst. Yearb. 67, 153–158.

Li, J.-P., O'Neill, H.S.C.., Seifert, F., 1995. Subsolidus Phase Relations in the System MgO-SiO2-Cr-O in Equilibrium with Metallic Cr, and their Significance for the Petrochemistry of Chromium. J. Petrol. 36, 107–132.

Miletich, R., Nowak, M., Seifert, F., Angel, R.J., Brandstätter, G., 1999. High-pressure crystal chemistry of chromous orthosilicate, Cr2SiO4. A single-crystal X-ray diffraction and electronic absorption spectroscopy study. Phys. Chem. Miner. 26, 446–459. https://doi.org/10.1007/s002690050207

Moynier, F., Yin, Q.-Z., Schauble, E., 2011. Isotopic evidence of Cr partitioning into Earth's core. Science 331, 1417–1420. https://doi.org/10.1126/science.1199597

Murck, B.W., Campbell, I.H., 1986. The effects of temperature, oxygen fugacity and melt composition on the behaviour of chromium in basic and ultrabasic melts. Geochim. Cosmochim. Acta 50, 1871–1887. https://doi.org/10.1093/petroj/40.5.831

Nesbitt, H.W., Young, G.M., 1984. Prediction of some weathering trends of plutonic and volcanic rocks based on thermodynamic and kinetic considerations. Geochim. Cosmochim. Acta 48, 1523–1534. https://doi.org/10.1016/0016-7037(84)90408-3

Nesbitt, H.W., Young, G.M., 1982. Early Proterozoic climates and plate motions inferred from major elements chemistry of lutites. Nature 299, 715–717.

Nicklas, R.W., Puchtel, I.S., Ash, R.D., 2018. Redox state of the Archean mantle: Evidence from V partitioning in 3.5–2.4 Ga komatiites. Geochim. Cosmochim. Acta 222, 447–466. https://doi.org/10.1016/j.gca.2017.11.002

Nicklas, R.W., Puchtel, I.S., Ash, R.D., 2016. High-precision determination of the oxidation state of komatiite lavas using vanadium liquid-mineral partitioning. Chem. Geol. 433, 36–45. https://doi.org/10.1016/j.chemgeo.2016.04.011

Nisbet, E.G., Arndt, N.T., Bickle, M.J., Chauvel, C., Cheadle, M., Martin, A., Renner, R., Roedder, E., Hegner, E., Kyser, T.K., 1987. Uniquely fresh 2 . 7 Ga komatiites from the Belingwe greenstone belt , Zimbabwe. Geology 15, 1147–1150.

Nisbet, E.G., Bickle, M.J., Martin, A., 1977. The Mafic and Ultramafic Lavas of the Belingwe, Rhodesia. J. Petrol. 18, 521–566.

Nisbet, E.G., Cheadle, M.J., Arndt, N.T., Bickle, M.J., 1993. Constraining the Potential Temperature of the Archean Mantle - a Review of the Evidence from Komatiites. Lithos 30, 291–307. https://doi.org/Doi 10.1016/0024-4937(93)90042-B

O'Neill, H.S.C., Berry, A.J., 2006. Activity coefficients at low dilution of CrO, NiO and CoO in melts in the system CaO-MgO-Al2O3-SiO2 at 1400°C: Using the thermodynamic behaviour of transition metal oxides in silicate melts to probe their structure. Chem. Geol. 231, 77–89. https://doi.org/10.1016/j.chemgeo.2006.01.004

Project, B.V.S., 1981. Basaltic Volcanism on the Terrestrial Planets.

Puchtel, I.S., Haase, K.M., Hofmann, A.W., Chauvel, C., Kulikov, V.S., Garbe-Schönberg, C.D., Nemchin, A.A., 1997. Petrology and geochemistry of crustally contaminated komatiitic basalts from the Vetreny Belt , southeastern Baltic Shield : Evidence for an early Proterozoic mantle plume beneath rifted Archean continental lithosphere. Geochim. Cosmochim. Acta 61, 1205–1222.

Puchtel, I.S., Hofmann, A.W., Mezger, K., Shchipansky, A.A., Kulikov, V.S., Kulikova, V. V., 1996. Petrology of a 2.41 Ga remarkably fresh komatiitic basalt lava lake in Lion Hills, central Vetreny Belt, Baltic Shield. Contrib. to Mineral. Petrol. 124, 273–290. https://doi.org/10.1007/s004100050191

Puchtel, I.S., Toubal, M., Blichert-Toft, J., Walker, R.J., Brandon, A.D., Nicklas, R.W., Kulikov, V.S., Samsonov, A. V., 2016a. Lithophile and siderophile element systematics of Earth ' s mantle at the Archean – Proterozoic boundary : Evidence from 2.4 Ga komatiites. Geochim. Cosmochim. Acta

180, 227–255. https://doi.org/10.1016/j.gca.2016.02.027

Puchtel, I.S., Touboul, M., Blichert-Toft, J., Walker, R.J., Brandon, A.D., Nicklas, R.W., Kulikov, V.S., Samsonov, A. V., 2016b. Lithophile and siderophile element systematics of Earth's mantle at the Archean-Proterozoic boundary: Evidence from 2.4 Ga komatiites. Geochim. Cosmochim. Acta 180, 227–255. https://doi.org/10.1016/j.gca.2016.02.027

Puchtel, I.S., Walker, R.J., Brandon, A.D., Nisbet, E.G., 2009. Pt-Re-Os and Sm-Nd isotope and HSE and REE systematics of the 2.7 Ga Belingwe and Abitibi komatiites. Geochim. Cosmochim. Acta 73, 6367–6389. https://doi.org/10.1016/j.gca.2009.07.022

Renner, R., Nisbet, E.G., Cheadle, M.J., Arndt, N.T., Bickle, M.J., Cameron, W.E., 1994. Komatiite Flows from the Reliance Formation , Belingwe Belt , Zimbabwe : I . Petrography and Mineralogy. J. Petrol. 35, 361–400.

Révillon, S., Arndt, N.T., Chauvel, C., Hallot, E., 2000. Geochemical study of ultramafic volcanic and plutonic rocks from Gorgona Island, Colombia: The plumbing system of an oceanic plateau. J. Petrol. 41, 1127–1153. https://doi.org/10.1093/petrology/41.7.1127

Révillon, S., Chauvel, C., Arndt, N.T., Pik, R., Martineau, F., Fourcade, S., Marty, B., 2002. Heterogeneity of the Caribbean plateau mantle source : Sr , O and He isotopic compositions of olivine and clinopyroxene from Gorgona Island. Earth Planet. Sci. Lett. 205, 91–106.

Roeder, P.L., Reynolds, I., 1991. Crystallization of Chromite and Chromium Solubility in Basaltic Melts. J. Petrol. 909–934.

Schauble, E., 2004. Applying stable isotope fractionation theory to new systems. Rev. Mineral. Geochemistry 55, 65. https://doi.org/10.2138/gsrmg.55.1.65

Schoenberg, R., Merdian, A., Holmden, C., Kleinhanns, I.C., Haßler, K., Wille, M., Reitter, E., 2016. The stable Cr isotopic compositions of chondrites and silicate planetary reservoirs. Geochim. Cosmochim. Acta 183, 14–30. https://doi.org/10.1016/j.gca.2016.03.013

Schoenberg, R., Zink, S., Staubwasser, M., von Blanckenburg, F., 2008. The stable Cr isotope inventory of solid Earth reservoirs determined by double spike MC-ICP-MS. Chem. Geol. 249, 294–306. https://doi.org/10.1016/j.chemgeo.2008.01.009

Schreiber, H.D., Haskin, L.A., 1976. Chromium in basalts: Experimental determination of redox staets and partitioning among synthetic silicate phases. Proc. Lunar Planet. Sci. Conf. 7, 1221–1259.

Shahar, A., Ziegler, K., Young, E.D., Ricolleau, A., Schauble, E.A., Fei, Y., 2009. Experimentally determined Si isotope fractionation between silicate and Fe metal and implications for Earth's core formation. Earth Planet. Sci. Lett. 288, 228–234. https://doi.org/10.1016/j.epsl.2009.09.025

Shaw, D.M., 1970. Trace element fractionation during anatexis. Geochim. Cosmochim. Acta 34, 237–243.

Shen, J., Fang, Z., Qin, L., Zhang, Q., Xiao, Y., Yu, H., 2016. High temperature inter-mineral Cr isotope fractionation : ionic model constraint and implication for mantle xenoliths from North China Craton. Goldschmidt Conf. Abstr. 2816.

Shen, J., Qin, L., Fang, Z., Zhang, Y., Liu, J., Liu, W., Wang, F., Xiao, Y., Yu, H., Wei, S., 2018. High-temperature inter-mineral Cr isotope fractionation : A comparison of ionic model predictions and experimental investigations of mantle xenoliths from the North China Craton. Earth Planet. Sci. Lett. 499, 278–290. https://doi.org/10.1016/j.epsl.2018.07.041

Shen, J., Xia, J., Qin, L., Carlson, R.W., Huang, S., Helz, R.T., Mock, T.D., 2019. Stable chromium isotope fractionation during magmatic differentiation: Insights from Hawaiian basalts and implications for planetary redox conditions. Geochim. Cosmochim. Acta. https://doi.org/10.1016/j.gca.2019.10.003

Shore, M., 1996. Cooling and crystallisation of komatiite lava flows (PhD thesis).

Siebert, J., Corgne, A., Ryerson, F.J., 2011. Systematics of metal – silicate partitioning for many siderophile elements applied to Earth ' s core formation. Geochim. Cosmochim. Acta 75, 1451–1489. https://doi.org/10.1016/j.gca.2010.12.013

Sossi, P.A., Eggins, S.M., Nesbitt, R.W., Nebel, O., Hergt, J.M., Campbell, I.H., O'Neill, H.S.C., Kranendonk, M. Van, Rhodri Davies, D., 2016. Petrogenesis and geochemistry of Archean Komatiites. J. Petrol. 57, 147–184. https://doi.org/10.1093/petrology/egw004

Sossi, P.A., Moynier, F., Zuilen, K. Van, 2018. Volatile loss following cooling and accretion of the Moon revealed by chromium isotopes. PNAS 115, 10920–10925. https://doi.org/10.1073/pnas.1809060115

Sossi, P.A., O'Neill, H.S.C., 2016. Liquidus temperatures of komatiites and the effect of cooling rate on element partitioning between olivine and komatiitic melt. Contrib. to Mineral. Petrol. 171, 1–25. https://doi.org/10.1007/s00410-016-1260-x

Sossi, P.A., St, H., Neill, C.O., 2017. The effect of bonding environment on iron isotope fractionation between minerals at high temperature. Geochim. Cosmochim. Acta 196, 121–143. https://doi.org/10.1016/j.gca.2016.09.017

Toplis, M.J., 2005. The thermodynamics of iron and magnesium partitioning between olivine and liquid: Criteria for assessing and predicting equilibrium in natural and experimental systems. Contrib. to Mineral. Petrol. 149, 22–39. https://doi.org/10.1007/s00410-004-0629-4

Tuller-Ross, B., Savage, P.S., Chen, H., Wang, K., 2019. Potassium isotope fractionation during magmatic differentiation of basalt to rhyolite. Chem. Geol. 525, 37–45. https://doi.org/10.1016/j.chemgeo.2019.07.017

Walker, R.J.., Storey, M., Kerr, A.C.., Tarney, J., Arndt, N.T., 1999. Implications of 187Os isotopic heterogeneities in a mantle plume : Evidence from Gorgona Island and Curacao. Geochim. Cosmochim. Acta 63, 713–728.

Walter, M.J., 1998. Melting of garnet peridotite and the origin of komatiite and depleted lithosphere. J. Petrol. 39, 29–60. https://doi.org/10.1093/petroj/39.1.29

Wang, K., Jacobsen, S.B., 2016. Potassium isotopic evidence for a high-energy giant impact origin of the Moon. Nature 538, 487–490. https://doi.org/10.1038/nature19341

Wood, B.J., Wade, J., Kilburn, M.R., 2008. Core formation and the oxidation state of the Earth: Additional constraints from Nb, V and Cr partitioning. Geochim. Cosmochim. Acta 72, 1415–1426. https://doi.org/10.1016/j.gca.2007.11.036

Xia, J., Qin, L., Shen, J., Carlson, R.W., Ionov, D.A., 2017. Chromium isotope heterogeneity in the mantle. Earth Planet. Sci. Lett. 464, 103–115. https://doi.org/10.1016/j.epsl.2017.01.045

Zhu, K., Sossi, P.A., Siebert, J., Moynier, F., 2019. Tracking the volatile and magmatic history of Vesta from chromium stable isotope variations in eucrite and diogenite meteorites. Geochim. Cosmochim. Acta. https://doi.org/10.1016/j.gca.2019.07.043

Figure

Click here to download high resolution image

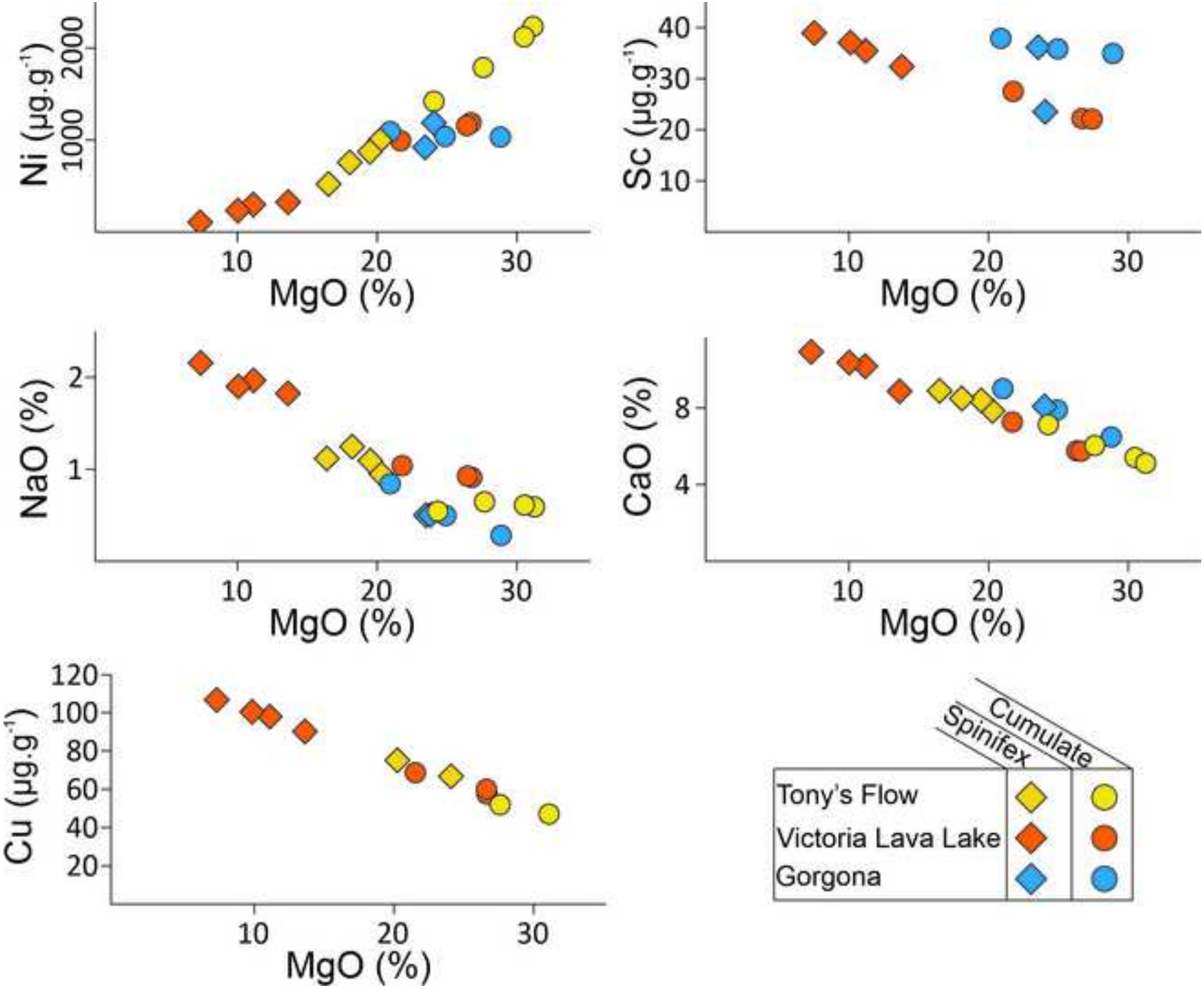

Figure 2

Click here to download high resolution image

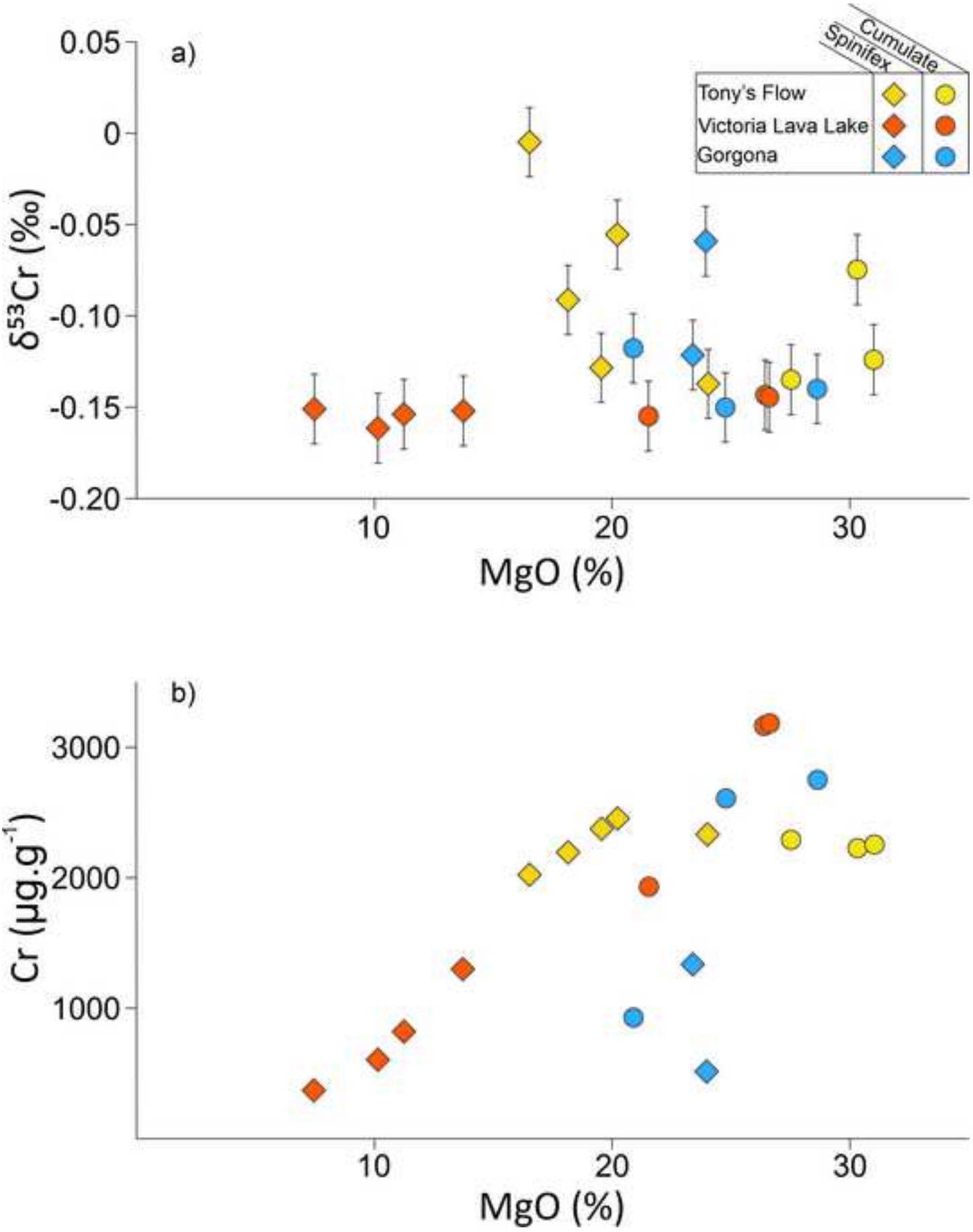

Figure 2

Click here to download high resolution image

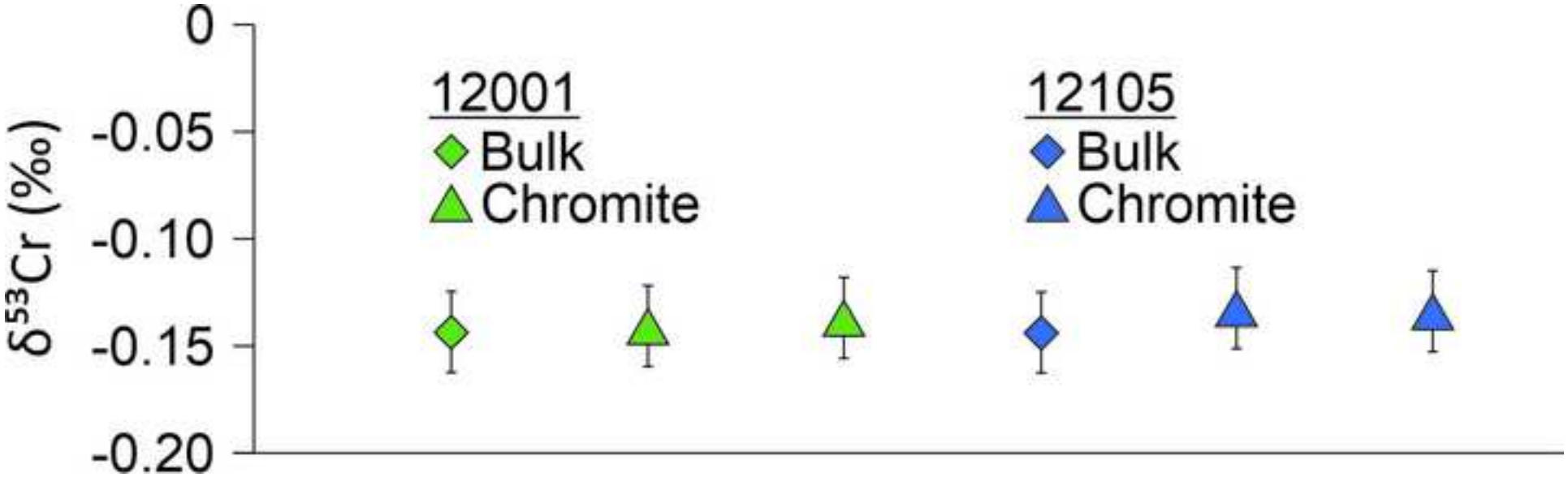

Figure 4

Click here to download high resolution image

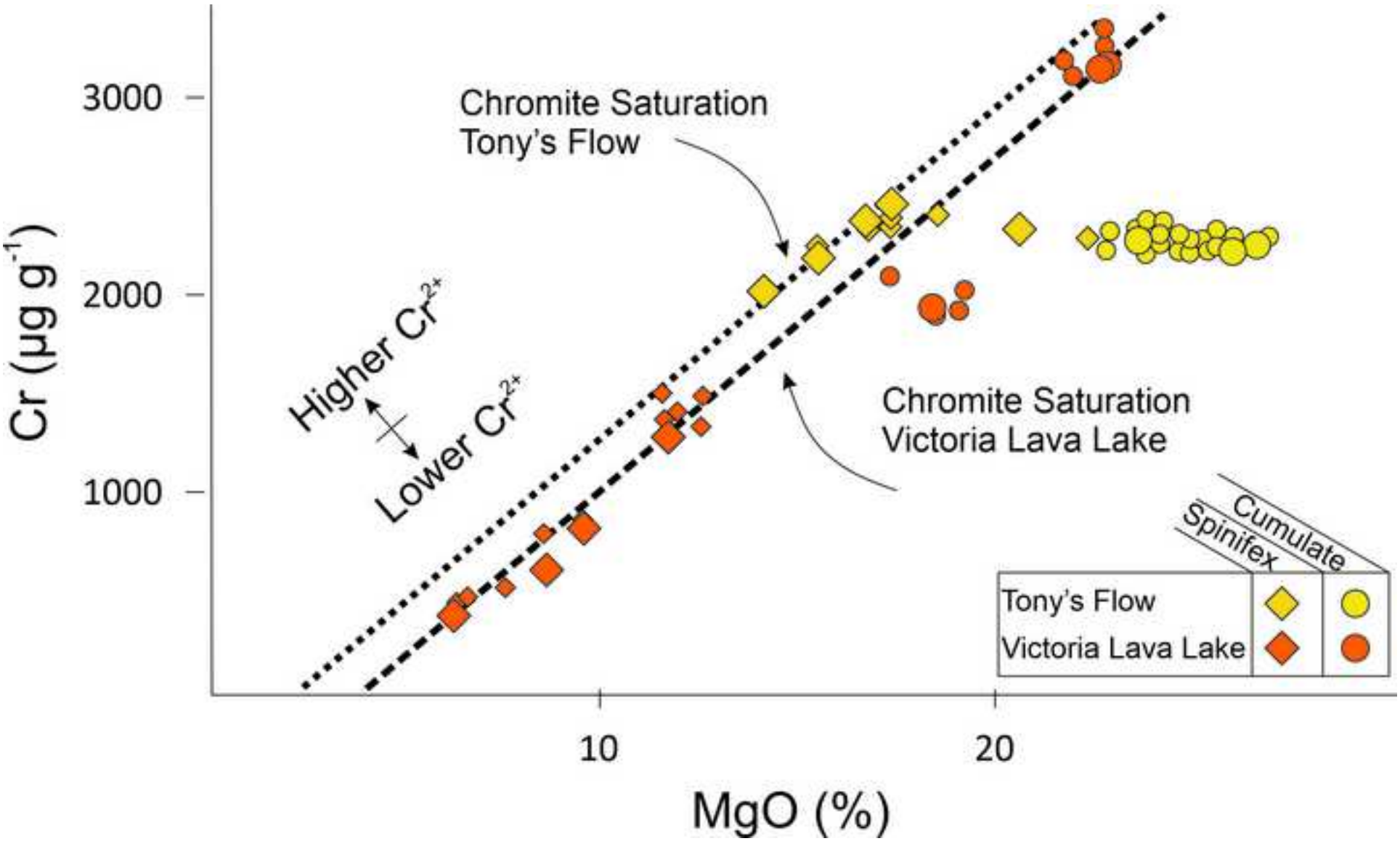

Figure 5

Click here to download high resolution image

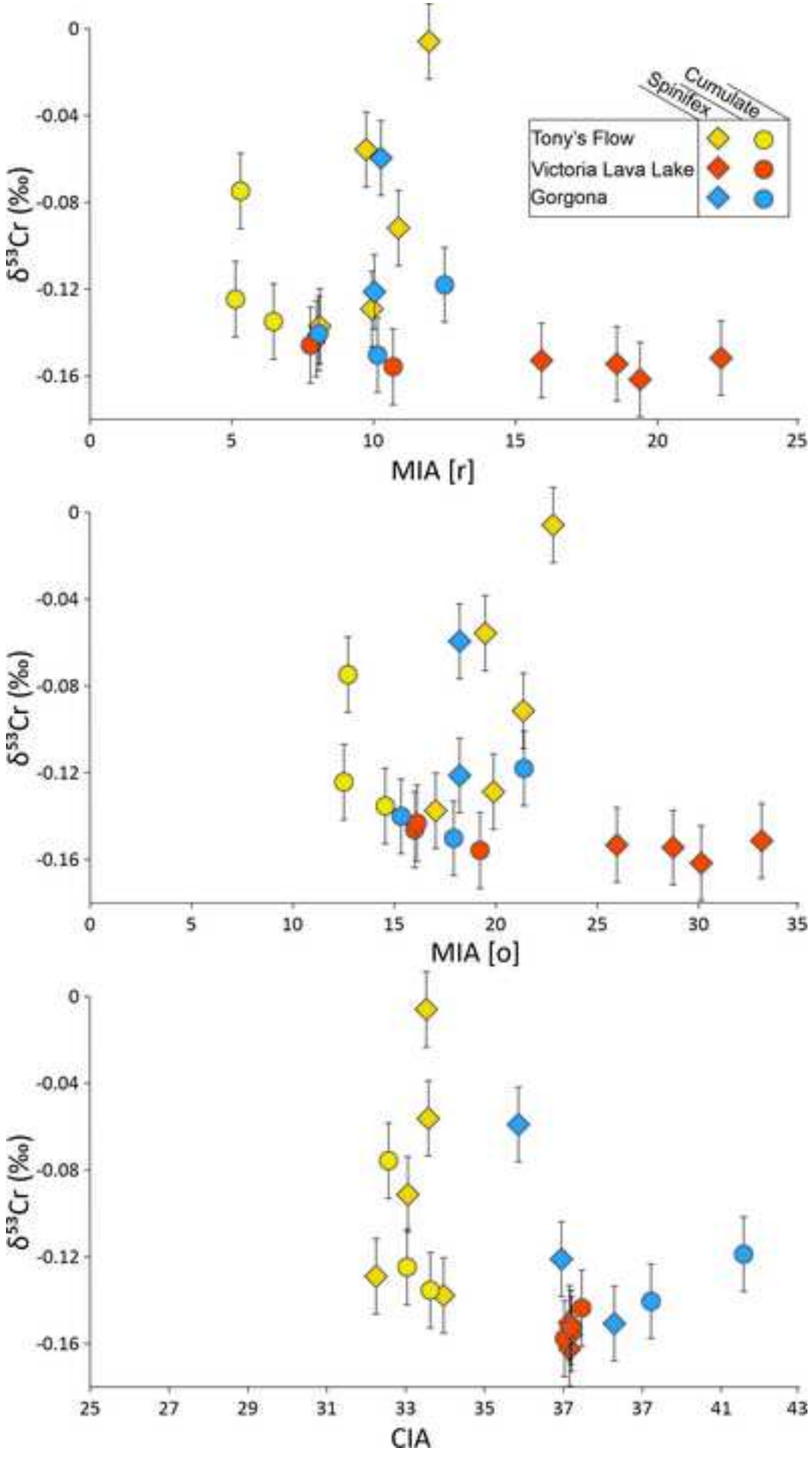

Figure 6

Click here to download high resolution image

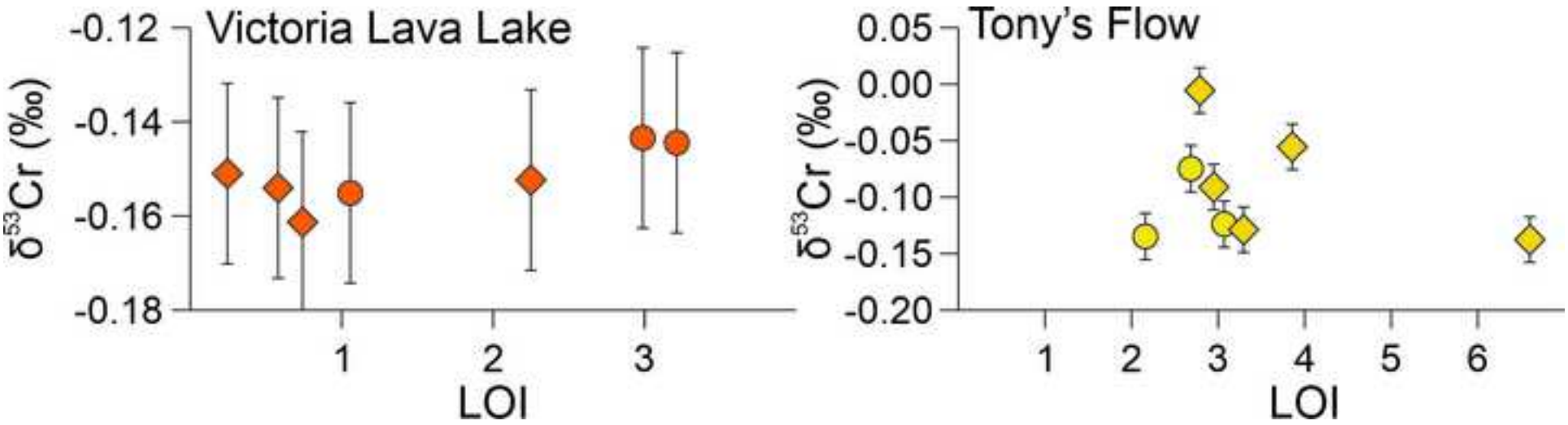

Figure 7

Click here to download high resolution image

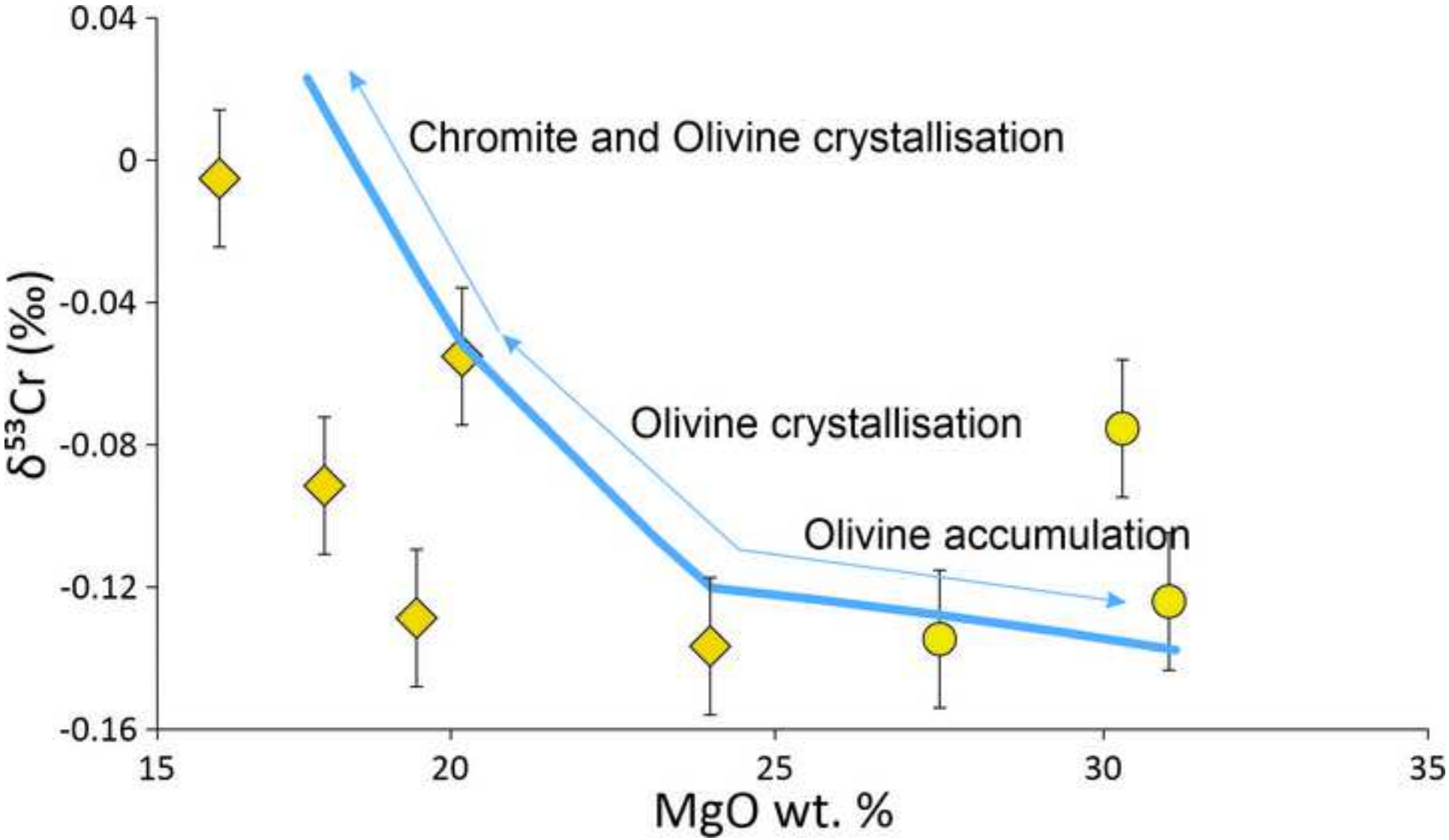

Figure 8

Click here to download high resolution image

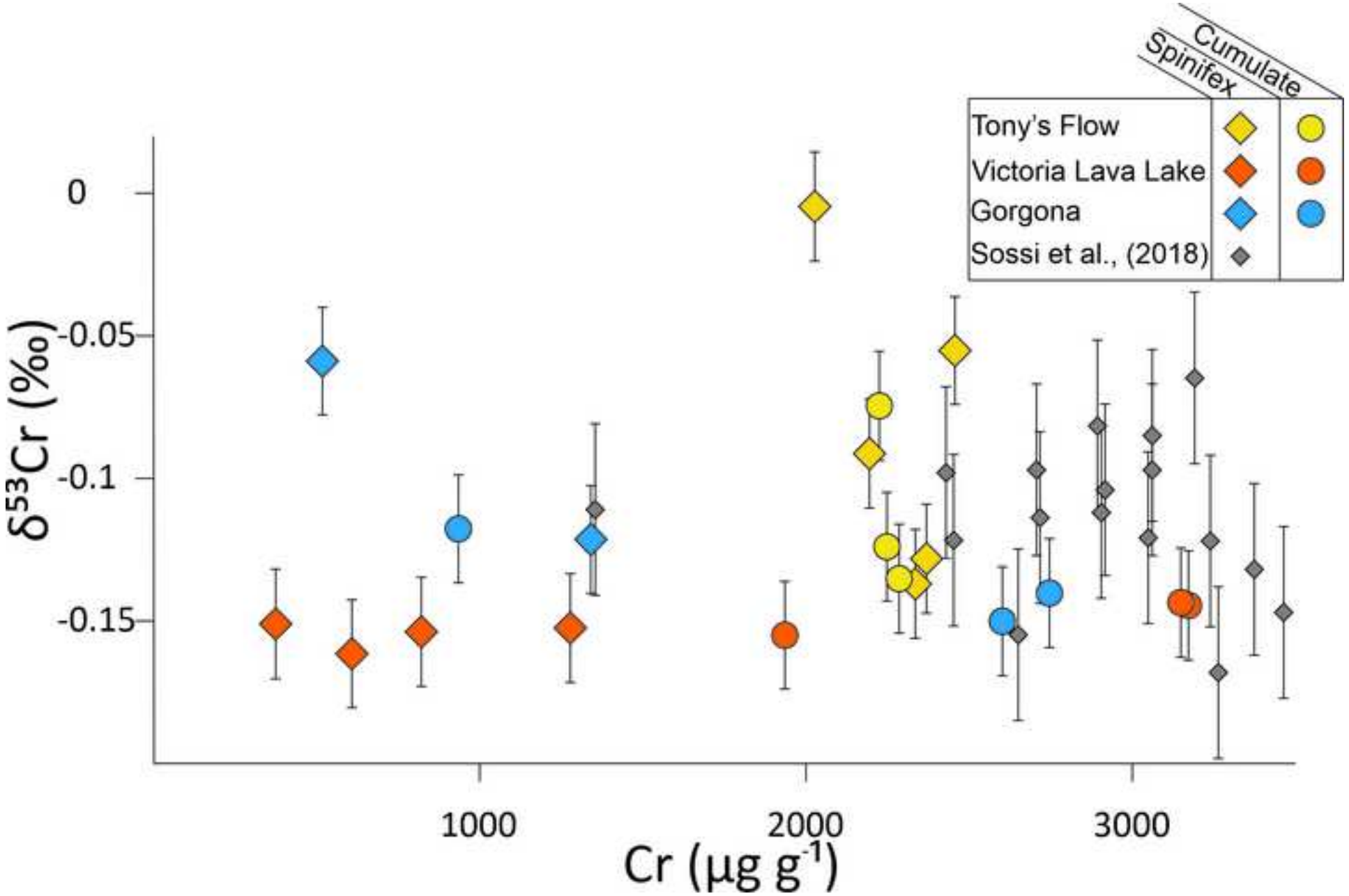

Figure 9

Click here to download high resolution image

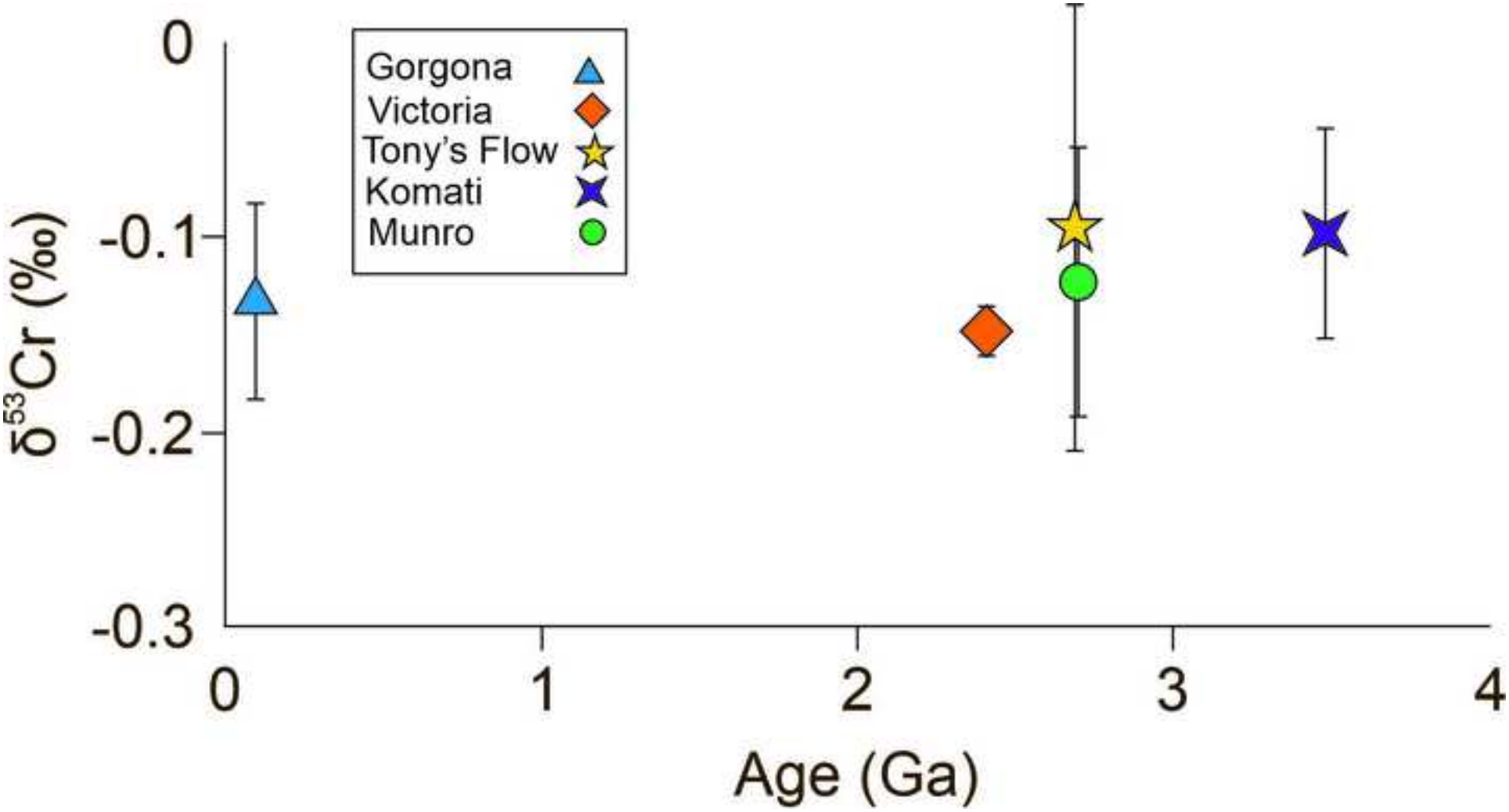

Figure and Table Captions

Figure 1

Figure 1. Compilation of komatiites adapted from Arndt (2008) and Barnes (1998). MgO and Cr variations of komatiites are explained by the accumulation and crystallisation of olivine and chromium. Accumulation of olivine increases the MgO content and decreases the Cr content, while crystalllisatino of olivine decreases MgO and increases Cr. Chromite accumulation leads to higher Cr concentrations with little change in the MgO content. The chromium content of the melt increases until the flow is saturated and chromite crystallisation begins.

Figure 2

Figure 2. Variations in δ^{53}Cr and [Cr] plotted against MgO (%), which can be used as a proxy of crystallisation. The δ^{53}Cr of all komatiite flows overlap. Resolvable variations in δ^{53}Cr are identified in Gorgona and Tony's Flow komatiites, while Victoria's Lava Lake has no change in Cr isotope composition. Gorgona and Tony's Flow show an increase in δ^{53}Cr at lower MgO (%). A positive correlation is seen between the [Cr] and MgO(%) at low MgO (%).

Figure 3

Figure 3. The δ^{53}Cr composition of whole-rock samples and chromite separates from the Victoria's Lava Lake. Note that both komatiites have indistinguishable Cr isotope compositions between the bulk rock and the chromites.

Figure 4

Figure 4. Comparison of chromite saturation curves of Tony's Flow and the Victoria's Lava Lake. Samples analysed in this study are represented with larger symbols. Tony's Flow has a chromite

saturation line that is depressed compared to the Victoria's Lava Lake. This is due to the higher temperatures within this flow, which causes Cr to be more soluble.

Figure 5

Figure 5. δ^{53}Cr plotted against indexes of chemical alteration, MIA[o], MIA[r] and CIA. Higher index values indicate the loss of mobile elements. No covariation occurs between the indexes and δ^{53}Cr.

Figure 6

Figure 6a and b showing δ^{53}Cr plotted against loss on ignition, an indicator of serpentinisation. No correlations are seen.

Figure 7

Figure 7. Fractional crystallisation and olivine accumulation model used to recreate the composition of Tony's Flow. In order to create the variation seen in the samples, olivine -0.2‰ lighter than the melt is required to form. The olivine accumulation is assumed to occur with a constant composition. This will not likely occur in nature, as olivine will form from an increasingly heavy melt, which will cause a flatter olivine accumulation line. At 21% chromite crystallisation occurs, as identified in Figure 2, with the partition coefficient is increased and the fractionation factor is decreased.

Figure 8

Figure 8. δ^{53}Cr variations against Cr concentrations. The Victoria's Lava Lake show no variations while Tony's Flow and Gorgona komatiites have heavier δ^{53}Cr at lower Cr concentrations. Samples measured here show δ^{53}Cr composition of komatiites similar to those from (Sossi et al., 2018). *Samples from Sossi et al., (2018) are all Archean spinifex komatiites. The high [Cr] of komatiites from Sossi et al., (2018), is due to these samples being spinifex-textured komatiites only.*

Figure 9

Figure 9. The weighted average $\delta^{53}Cr$ composition of the mantle through time based on five komatiite flows. The composition of the komatiite flows is similar over the history of the Earth.

Table 1. Cr isotopic composition and Cr concentrations of komatiites and chromite separates

Chromium concentration data were (a) adopted from (Puchtel et al., 2016, 2009)*, (b) through analysis using the Department of Earth Sciences, Oxford, PerkinElmer NexION 350D Quadrople ICP-MS, or (c) by isotope dilution during the deconvolution of the double spike. An expanded data table is provided in the Appendix 2.*

Table 2 BSE estimates through different methods

Table 2 recreated komatiite flow compositions using two different methods. The weighted average is able to best account for $\delta^{53}Cr$ variations during crystallisation.

Table 1. Cr isotopic composition and Cr concentrations of komatiites and chromite separates

Sample	Location	Type	$\delta^{53}Cr$	2 s.e.	Cr (µg g^{-1})	MgO (%)
GOR 94-3	Gorgona	Cumulate	-0.14	0.01	2745[b]	28.6
GOR 94-17	Gorgona	Cumulate	-0.12	0.01	932[b]	20.9
GOR 94-44	Gorgona	Cumulate	-0.15	0.01	2598[b]	24.7
GOR 94-19	Gorgona	Spinifex	-0.06	0.02	514[b]	23.9
GOR 94-43	Gorgona	Spinifex	-0.12	0.01	1340[b]	23.4
TN-16	Tony's Flow	Cumulate	-0.12	0.01	2247[a]	31.0
TN-19	Tony's Flow	Cumulate	-0.07	0.01	2223[a]	30.3
ZV-10	Tony's Flow	Cumulate	-0.14	0.01	2284[a]	27.5
TN-01	Tony's Flow	Spinifex	-0.14	0.03	2332[a]	24.0
TN-03	Tony's Flow	Spinifex	-0.06	0.01	2455[a]	20.2
TN-05	Tony's Flow	Spinifex	-0.13	0.01	2369[a]	19.5
TN-06	Tony's Flow	Spinifex	-0.09	0.01	2191[a]	18.1
ZV-14	Tony's Flow	Spinifex	-0.01	0.01	2023[a]	16.5
12001	Victoria's Lava Lake	Cumulate	-0.14	0.01	3146[a]	26.4
12105	Victoria's Lava Lake	Cumulate	-0.14	0.01	3170[a]	26.6
12106	Victoria's Lava Lake	Cumulate	-0.15	0.01	1933[a]	21.5
12101	Victoria's Lava Lake	Spinifex	-0.16	0.01	607[a]	10.5
12110	Victoria's Lava Lake	Spinifex	-0.15	0.01	1277[a]	13.7
12117	Victoria's Lava Lake	Spinifex	-0.15	0.02	818[a]	11.2
12124	Victoria's Lava Lake	Spinifex	-0.15	0.01	372[a]	7.4
12001 Chr 1	Victoria's Lava Lake	Chromite	-0.14	0.01	242,400[c]	-
12001 Chr 2	Victoria's Lava Lake	Chromite	-0.14	0.04	239,000[c]	-
12105 Chr 1	Victoria's Lava Lake	Chromite	-0.13	0.02	202,200[c]	-
12105 Chr 2	Victoria's Lava Lake	Chromite	-0.13	0.02	249,800[c]	-

Chromium concentration data were (a) adopted from (Puchtel et al., 2016, 2009)*, (b) through analysis using the Department of Earth Sciences, Oxford, PerkinElmer NexION 350D Quadrople ICP-MS, or (c) by isotope dilution during the deconvolution of the double spike. An expanded data table is provided in the appendix 2.*

Table 2 BSE estimates through different methods

Method	Victoria Lava Lake	Tony's Flow	Gorgona	Komati	Munro	BSE
Closest Composition	-0.15	-0.14	-0.12	-0.08	-0.17	-0.13 ± 0.06 ‰
Weighted average	-0.15	-0.10	-0.13	-0.11	-0.13	-0.12 ± 0.04‰

Table 2 recreated komatiite flow compositions using two different methods. The weighted average is able to best account for $\delta^{53}Cr$ variations during crystallisation.

Background dataset for online publication only

Click here to download Background dataset for online publication only: Appendix 1.docx

Background dataset for online publication only

Click here to download Background dataset for online publication only: Appendix 2.xlsx

***Declaration of Interest Statement**

Declaration of interests

☒ The authors declare that they have no known competing financial interests or personal relationships that could have appeared to influence the work reported in this paper.

☐The authors declare the following financial interests/personal relationships which may be considered as potential competing interests: